UILU-ENG-87-2550

SINGLE-COLOR LASER RANGING WITH A CUBE-CORNER-RETROREFLECTOR ARRAY

by

G. Hugh Song

EOSL No. 87-004

Technical Report
June 1987

Supported by
Contract No. NASA NSG-5049

NATIONAL AERONAUTICS & SPACE ADMINISTRATION
Goddard Space Flight Center
Greenbelt, Maryland 20771

ELECTRO-OPTIC SYSTEMS LABORATORY
DEPARTMENT OF ELECTRICAL AND COMPUTER ENGINEERING
COLLEGE OF ENGINEERING
UNIVERSITY OF ILLINOIS
URBANA, ILLINOIS 61801

TABLE OF CONTENTS

PART I. LIDAR CROSS SECTION OF A TILTED CUBE-CORNER RETROREFLECTOR

ABSTRACT

Lidar cross section of some typical types of cube-corner retroreflectors (CCR's) having a three corner mirror system is investigated for the case that the CCR is tilted from the normal illumination axis. Analytic expressions for the effective aperture area for the two typical window types (circular and hexagonal) of CCRs are obtained for the case that the CCR is tilted. The range of incidence angle in which only the total reflection occurs at all three uncoated corner mirrors has been found to vary considerably with the orientation of CCR and the refractive index of the CCR prism. The analytical expression for the far-field diffraction pattern of a tilted CCR is obtained by taking different polarization transformation of the six sectors of the effective reflecting aperture into account. This expression is essential when evaluating the lidar cross section of a moving CCR which is tilted in general. Formulas for the angles defining the six sectors have also been obtained.

I. INTRODUCTION

Analysis of the lidar cross section of a cube corner retroreflector (CCR) has become important under the enlightenment of its use in ranging satellites [1] and on the moon [2]. There are various types of CCRs or array of CCRs. It may be designed to have a hexagonal, triangular, or circular front view. According to the existence of coating on the triple-corner-mirror system, they may be classified to coated-mirror CCRs for wider retroreflecting solid angle and uncoated-mirror CCRs for better reflectivity and longer life in space. According to the array shape of CCRs, there are honey-comb array (retroreflectors for traffic signs and automobiles), flat array (on the moon), spherical array (e.g., the Laser Geodynamic Satellite (LAGEOS)), etc. Some CCRs have an intentional dihedral angle error for diffusing the reflected beam. In every case, lidar cross section analysis gives us some ideas on how to analyze the signal received from existing CCR arrays and on how to design those new CCRs.

We shall consider the lidar cross section of a single CCR whose front view is either circular or hexagonal, whose triple-mirror system is either coated or uncoated. To this end, the range of effective angle of incidence and the area of effective retroreflecting aperture is found. The far-field diffraction effect will also be considered as well as the velocity aberration effect. The analytical expression of the far-field diffraction pattern is obtained for a tilted CCR in terms of the Kirchhoff integral of the complex amplitudes of two linear orthogonal polarizations transformed while being reflected. The effective reflecting aperture over which the Kirchhoff integral should be carried is divided into six sectors having their own transformation matrices. It is a generalization of the work of Chang et al. [2] who obtained the expression of the diffraction pattern for a normally illuminated CCR with a

circular face. Throughout this work the effect of dihedral angle error is assumed to be nonexistent.

II. EFFECTIVE RETROREFLECTING APERTURE AND REFLECTIVITY

Suppose a CCR with a circular front window, sometimes called a cylindrical CCR, is tilted from the normal illumination. That is, light enters the CCR with the entrance angle Φ. Then, the portion of effective retroreflecting aperture looks like Fig. 1 if we look at the CCR along the illumination axis, and its area is given by

$$A(\Phi) = 2a^2 \left[\cos^{-1}\left(\frac{d}{a}\tan\phi\right) - \frac{d}{a}\tan\phi\sqrt{1 - \left(\frac{d}{a}\right)^2\tan^2\phi}\right]\cos\Phi, \tag{1}$$

$$\phi = \sin^{-1}\left(\frac{\sin\Phi}{n}\right), \tag{2}$$

where a is the radius of the circular face and d is the depth of the vertex from the front face. n is the refractive index of the CCR prism. For the front face to be circular, $d \geq \sqrt{2}a$. Usually $d = \sqrt{2}a$ is chosen for maximum $A(\Phi)$ and henceforth we shall assume this configuration for a CCR with a circular face. The formula for $d = \sqrt{2}a$ was given in Ref.[1]. Note that the reflectivity and the area of the effective reflecting aperture are important factors that determine retroreflectance in the near-field. In fact, if the triple-corner-mirror system in a CCR is coated with metal, the reflectivity depends on the kind of metal as well as on the angle of incidence and the polarization of the incident light. Whereas, if corner mirrors are uncoated the reflectivity depends on whether the condition of the total reflection is satisfied or not inside the CCR prism. If total reflection occurs three times

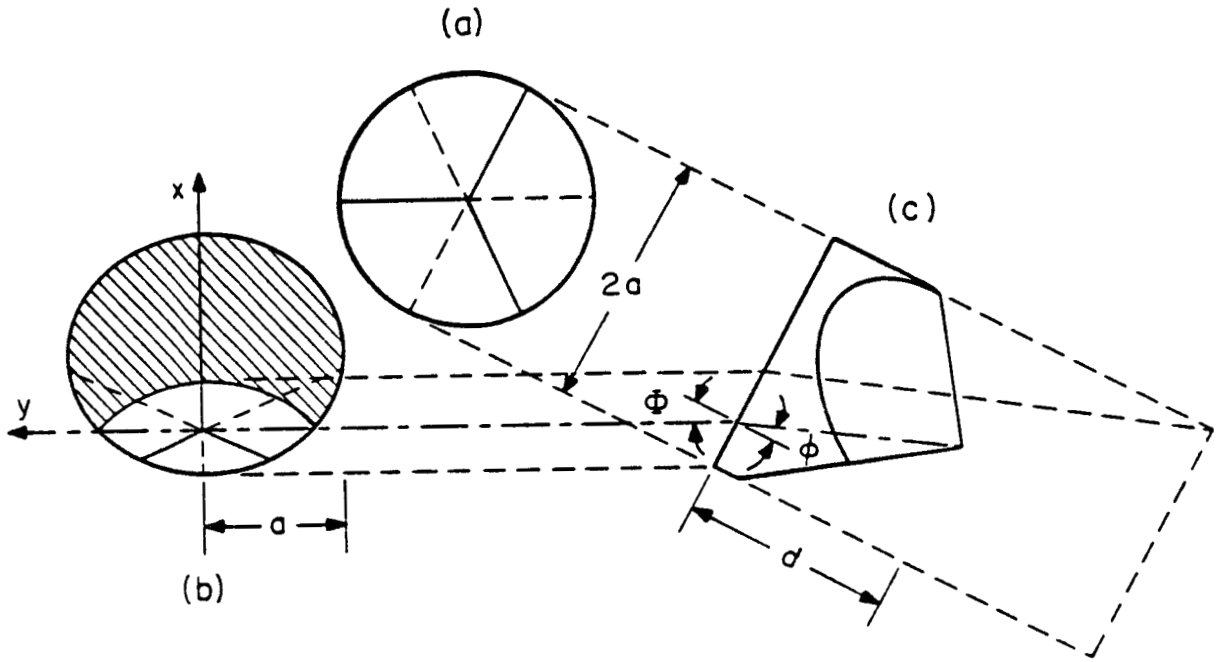

Figure 1. Two front views and the side view of a cube-corner retroreflector with a circular face, a) the front view when the observation axis is coincident with the reference axis which is perpendicular to the window face, b) the front view when the observation axis is tilted from the reference axis. The effective reflecting aperature is shown unhatched with the coordinates (x,y) whose origin is at the vertex seen through the window face, c) the side view with the image (dashed) of the front window that would be seen inside through itself.

consecutively inside the CCR prism, the reflectivity is unity during those three reflections. Hence the light intensity is only attenuated as light transmits into and out of the CCR prism through the front face. However, if the condition of the total reflection is not satisfied at one of the three reflections, the reflectivity drops to a negligibly small fraction and considerable light intensity passes through that surface. Such a negligibly small fraction of retroreflection is due to the Fresnel reflection at the corner mirror where total reflection does not happen.

Here we shall consider the condition of the total reflection associated with the direction of the illumination axis and the orientation of a CCR. We define various directions and their corresponding angles as they are shown in Fig. 2. For simplicity, we shall assume that there is no dihedral angle error, that is, the three corner mirrors are at right angle to each other. To find the condition of the total reflection we have to find the incidence angle of light with respect to each of the three corner mirrors where the light is reflected consecutively inside the CCR prism. Two angles are given — Φ, the incidence angle of light illumination on the front window, and γ, the azimuth angle measured from the direction to one of the three azimuths for the three edges of a CCR. At each edge two corner mirrors intersect. Given these two angles, we can find α and β, the latitude and longitude, respectively, in the spherical coordinate system (Appendix A).

$$\sin\alpha = \frac{1}{\sqrt{3}} (\cos\phi + \sqrt{2}\sin\phi\cos\gamma), \qquad 0 < \alpha < \pi/2, \tag{3}$$

$$\cos(\beta - \frac{\pi}{4}) = \frac{\sqrt{3}\cos\phi - \sin\alpha}{\sqrt{2 - 2\sin^2\alpha}}, \qquad 0 < \beta < \pi/2, \tag{4}$$

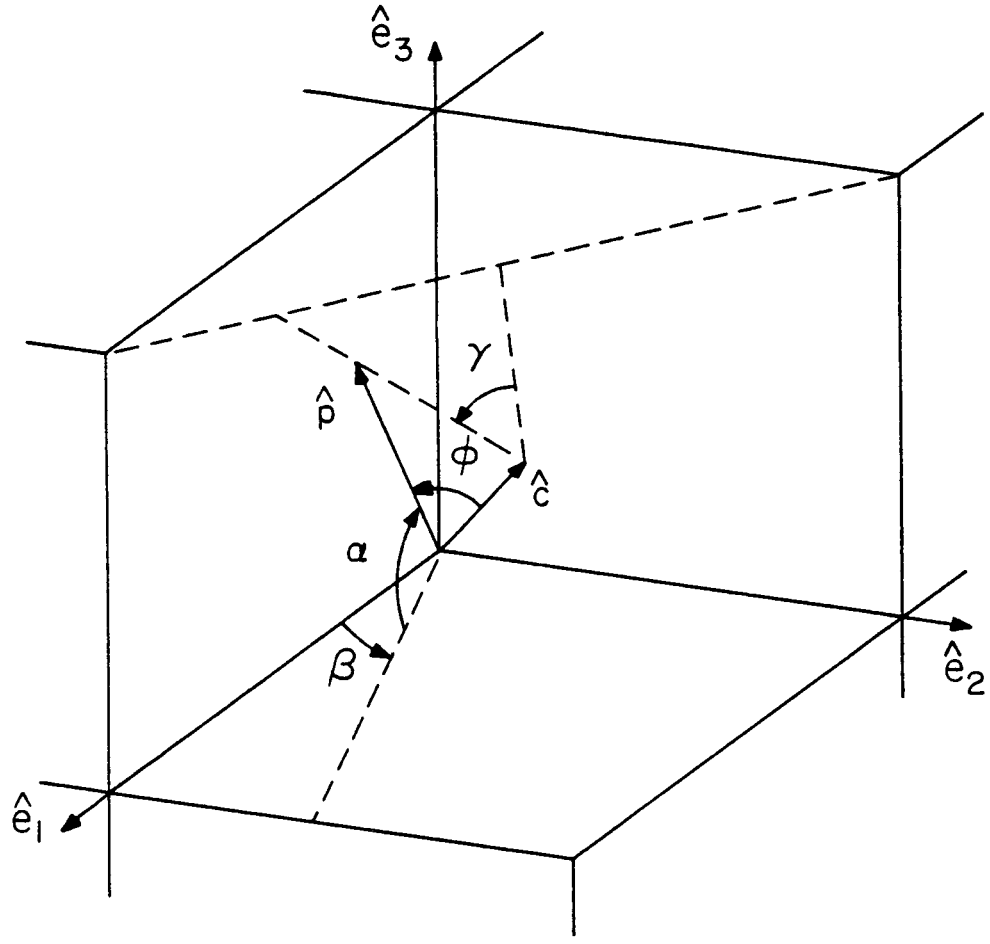

Figure 2. Coordinate system for a cube-corner retroreflector. Various angles and directions are depicted as it would be seen by an observer inside the reflector prism. The reference-axis unit vector is denoted by $\hat{c}$.

where ϕ is the refracted angle inside the CCR prism given in Eq. (2). We may also find cosine of the incidence angles of light on the three corner-mirror planes. They are $\sin\alpha$ for the mirror plane placed horizontally in the coordinate system shown in Fig. 2, and $\cos\alpha\cos\beta$ and $\cos\alpha\sin\beta$ for the two mirrors placed vertically and at right angle to each other. When the corner mirrors are not coated, all of these three values of cosine should be less than $\sqrt{1 - 1/n^2}$, cosine of the critical angle of total reflection, to ensure the total reflection. That is,

$$\cos\psi_1 = \cos\alpha\cos\beta < \sqrt{1 - 1/n^2}, \tag{5}$$

$$\cos\psi_2 = \cos\alpha\sin\beta < \sqrt{1 - 1/n^2}, \tag{6}$$

$$\cos\psi_3 = \sin\alpha < \sqrt{1 - 1/n^2}, \tag{7}$$

These three inequalities determine the retroreflecting angle range of the incidence angle Φ at a specific orientation of the CCR. Only one of the three incidence angles does not satisfy the condition when the three inequalities are not satisfied in all. Let this incidence angle be ψ_m. Then for the TE polarization whose electric field is parallel to the mirror plane and the TM polarization which is orthogonal to TE, the reflection coefficients for the electric field amplitude are

$$\rho_{TM}(\psi_m) = \frac{\tan(\psi_m - \Psi_m)}{\tan(\psi_m + \Psi_m)}, \quad \rho_{TM}(\psi_m) = -\frac{\sin(\psi_m - \Psi_m)}{\sin(\psi_m + \Psi_m)} \tag{8}$$

respectively, where $\Psi_m = \sin^{-1}(n \sin\psi_m)$.

If we neglect the retroreflection by multiple-order reflection inside the CCR prism. The first-order reflectivity of an uncoated-mirror CCR is determined by the attentuation when light passes through the front window in

and out. This attentuation depends on the polarization of the incident light and on the existence of antireflection coating. Here we shall not include the effect of antireflection coating in our analysis. For the TE polarization whose electric field is parallel to the front window and the TM polarization which is orthogonal to TE, the transmission coefficients for the electric field amplitude as it enters the CCR are [3]

$$t^{in}_{TE}(\Phi) = \frac{2\cos\Phi}{\cos\Phi + n\cos\phi}, \qquad t^{in}_{TM}(\Phi) = \frac{2\cos\Phi}{n\cos\Phi + \cos\phi} \tag{9}$$

respectively. Those coefficients for the light coming out are

$$t^{out}_{TE}(\Phi) = \frac{2n\cos\phi}{n\cos\phi + \cos\Phi}, \qquad t^{out}_{TM}(\Phi) = \frac{2n\cos\phi}{\cos\phi + n\cos\Phi} \tag{10}$$

Here we have not considered the polarization change brought about during the three consecutive total reflections at the three corner mirrors. It is expected that the retroreflected light will come out of the front window with six different polarizations depending on the location where the light comes out [2]. One may observe those six sectors that look like pie cuts as he sees through a tilted CCR.

For a given aspect of the CCR, there are three incidence angles, ψ_1, ψ_2, and ψ_3 inherent to the reflections at the three corner mirrors regardless of their order of reflection. However, light comes out with six different polarization states according to the six different permutations of the three internal reflections. It is just as a series of different birefingence plates do not commute unless their corresponding two orthogonal eigenpolarization states coincide between the plates [4].

If the triple-mirror system is coated with metal, e.g., aluminum or silver, the expression for the attenuation in this case will be rather complicated than the case of an uncoated CCR, and the result may be inaccurate unless very accurate data of the conductivity and the dielectric constant of the metal at the wavelength of the light being used is provided.

Most CCRs that are used as retroreflectors in vehicles or for traffic signs have a hexagonal front view and form a flat honeycomb-like array made of plastics without rear-side coating. Hence the knowledge on the effective reflecting area $A(\Phi,\gamma)$ of a tilted CCR with a hexagonal front window is needed for the calculation of its retroreflectance. The method for finding the effective reflecting area of a tilted CCR is found in Refs.[5] and [6]. Based on this method, we can find explicit expressions for its computation as follows. We can easily find that there is a hexagonal symmetry for the condition of total reflection and thus for the computation of the effective retroreflecting area. So we may consider only one of six equivalent sectors after transforming the given azimuth angle into an equivalent azimuth γ' in this sector. By choosing this sector in $0 < \gamma' < \pi/3$, the transformation is given by

$$\gamma' = \min(|\gamma|,\ |\gamma-2\pi/3|,\ |\gamma-4\pi/3|)\ . \tag{11}$$

Then by the rule given in Eqs.(3) and (4) we can find a new set of angles, α' and β', from ϕ and γ'. Next, according to the value of $\tan\alpha'$, we can find the effective retroreflecting aperture area normalized to the case of normal incidence ($\Phi = 0$). (Appendix B)

$$\frac{A(\Phi,\gamma)}{A(0,\gamma)} = \frac{\cos\Phi}{\sqrt{3}\,\sin\phi} \times \begin{cases} 2\sin 2\beta' \cos\alpha' \cot\alpha', \\ \quad \text{for } 2\cos\beta' \leq \tan\alpha', \\ \sin\beta' (4\cos\alpha' - \sin\alpha'/\cos\beta'), \\ \quad \text{for } \cos\beta' \leq \tan\alpha' \leq 2\cos\beta', \\ \sin\beta' \cos\alpha' (4 - \cos\beta' \cot\alpha'), \\ \quad \text{for } \sin\beta' \leq \tan\alpha' \leq \cos\beta'. \end{cases} \tag{12}$$

Actually $\tan\alpha' < 1/\sqrt{2}$ is preexcluded from the possible range of the angle α' that the first sector can take. In Fig. 3, this effective retroreflecting aperture area and the beam reflectivities are plotted in Fig. 3 for two sample azimuthal directions of a CCR by varying the entrance angle. They are plotted for two types of CCRs; the one having a circular face with the refractive index $n = 1.455$ of quartz and the other having a hexagonal face with $n = 1.5$ of plastics. The beam reflectivity is the absolute square of the product of the two kinds of transmission coefficients in Eqs. (9)-(10) and the reflection coefficient in Eq. (8). The last coefficient may not be considered when total reflection only occurs in the triple-mirror system. The FORTRAN program for computing and plotting such area or the beam retroreflectivity of the foregoing two typical types of CCRs is given in Appendix C.

The near-field retroreflectance of a CCR with an uncoated corner-mirror system can be found by multiplying the effective reflecting aperture area and beam reflectivity of light passing through the front window and then normalizing it with respect to the case of normal incidence.

As one can easily see, the effective reflecting area does not vary so much with the varying azimuth angle. However, it varies considerably with the entrance angle. Moreover, when the CCR has uncoated corner mirrors, the acceptance angle range in which only the total reflection occurs at the triple-corner-mirror system varies considerably according to the orientation of the

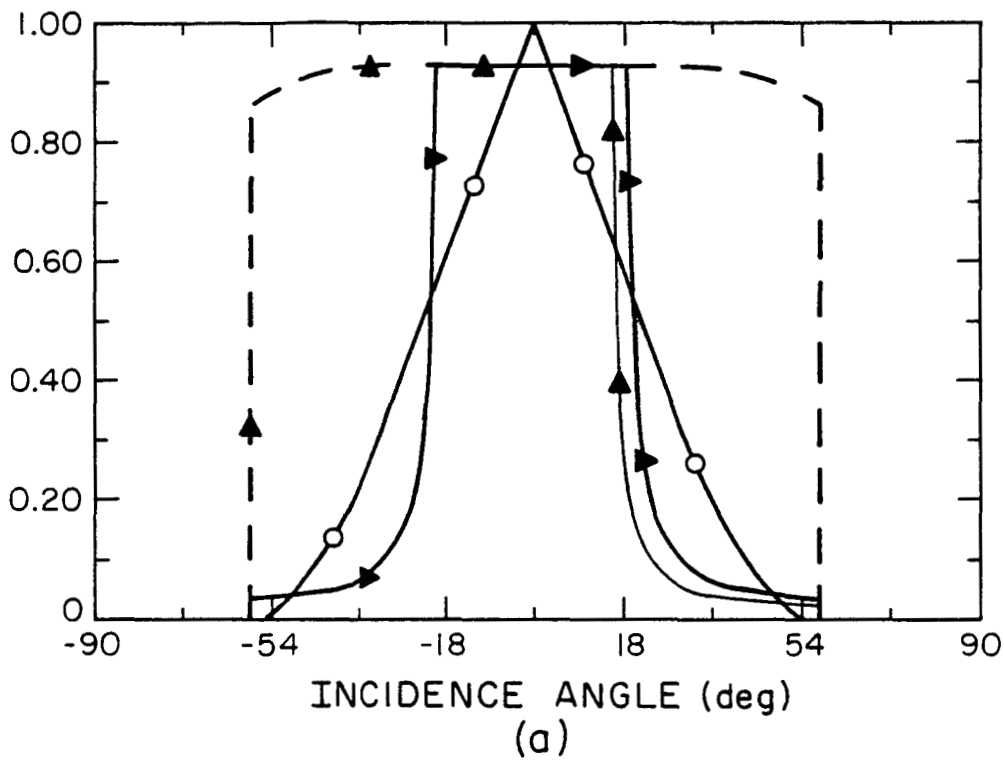

Figure 3. (a) The variations of the normalized effective retroreflecting aperture area and the beam reflectivity with the varying entrance angle Φ for the cube-corner retroreflector with a circular face. The refractive index has been set at n = 1.455 of quartz. Two sample asimuth angles $\gamma = 0^{o}$ and 90^{o} from one edge direction have been chosen. -o-o- The common effective retroreflecting aperture area for both azimuths. ▸▸ [▲▲] The beam reflectivity for $\gamma = 0^{o}$ [$\gamma = 90^{o}$] when the triple mirror system is uncoated. --- The beam reflectivity for both azimuths when the triple-mirror system is coated. (b) Those variations for the one having a hexagonal face. The refractive index has been set at 1.5. ▷▷ [△△] The effective retroreflecting aperture apea for $\gamma = 0^{o}$ [$\gamma = 90^{o}$]. ▸▸ [▲▲] The beam reflectivity for $\gamma = 0^{o}$ [$\gamma = 90^{o}$] when the tripple-mirror system is uncoated. -▸▸- [▲▲] The beam reflectivity for $\gamma = 0^{o}$ [$\gamma = 90^{o}$] when the tripple-mirror system is coated.

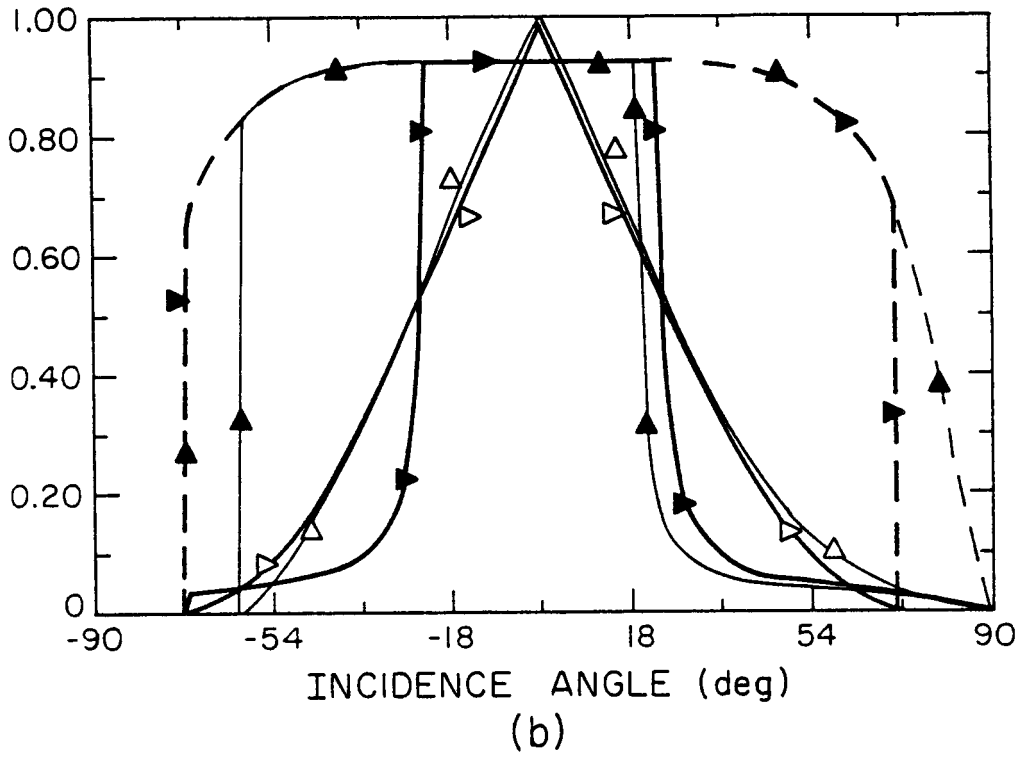

Figure 3. (continued)

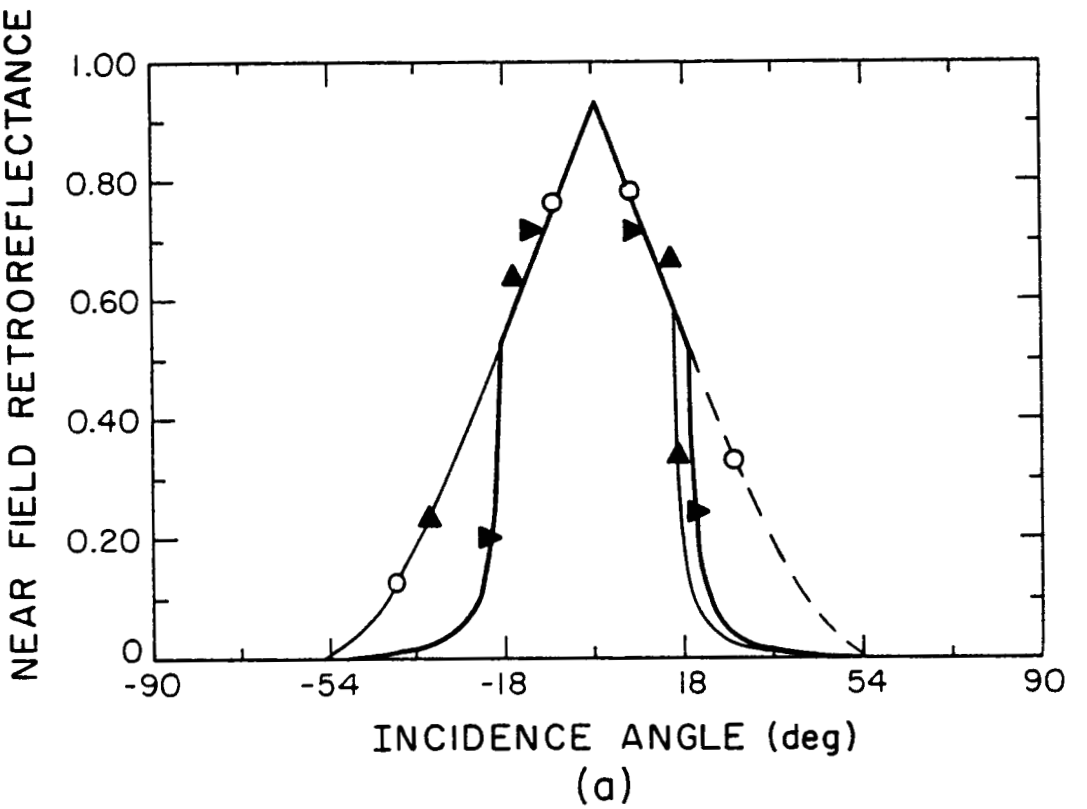

Figure 4. Variations of the near field retroreflectance for the two types of corner-cube retroreflectors considered in Fig. 3 (a) and (b).
(a) The one with a circular face (n = 1.455)
▸▸ [▲▲] for $\gamma = 0^{o}$ [$\gamma = 90^{o}$] when uncoated
·o·o· for both azimuths when coated
(b) The one with a hexagonal face (n = 1.5)
▸▸ [▲▲] for $\gamma = 0^{o}$ [$\gamma = 90^{o}$] when uncoated
·▷▷-[Δ-Δ] for $\gamma = 0^{o}$ [$\gamma = 90^{o}$] when coated.

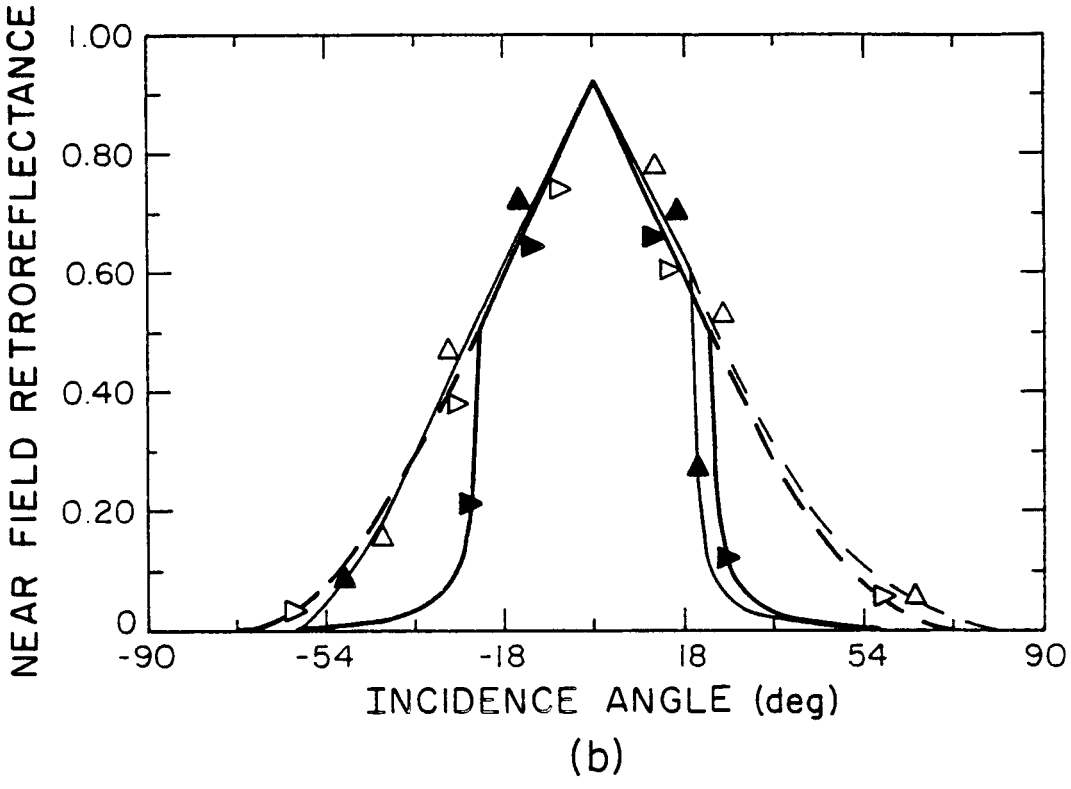

Figure 4. (continued)

CCR and the refractive index of the CCR prism. In Fig. 5, the maximum allowable entrance angle for the three cases of retroreflection by the two front-view types of a CCR is plotted as we vary the azimuth angle γ. The FORTRAN program that computes the maximum entrance angle is the program CRITANG, and CRITGRM plots it. They are shown in Appendix C.

III. LIDAR CROSS SECTION IN THE FAR-FIELD WITH THE VELOCITY ABBERATION EFFECT

If the CCR is far away from the receiver, we have to consider the diffraction of the reflected beam. For a rough estimate, when a circular aperture of diameter 2.54 cm is illuminated perpendicularly by light of wavelength 6943 A, the first zero in the far-field diffraction pattern occurs at 6 arcseconds off-axis from the reference axis. The broader the diffracted beam, the less peak power we can detect at a receiving point. If the CCR is tilted with respect to the illumination axis, the diffraction pattern becomes broader with the less receiving power. A small dihedral angle error may make the diffraction pattern irregular, which also decreases the receiving power. If the CCR target has a velocity to the direction right to the illumination axis, finite round-trip time induces the velocity aberration effect that displaces the maximum of the diffraction pattern from the illumination axis.

In this section, we shall investigate the diffraction pattern of a tilted CCR having a circular window, since most CCR arrays being used in space are of this type. The diffraction analysis of a tilted CCR has its worth when we consider, at the same time, the decrease in receiving power due to the velocity aberration effect of the moving target, i.e., the ranging satellite. The far-field diffraction pattern for the case of normal incidence to a CCR with a circular front window was investigated by Chang et al. [2]. They were concerned with the flat rectangular array of CCRs such as the array on the moon, which always faces to the earth.

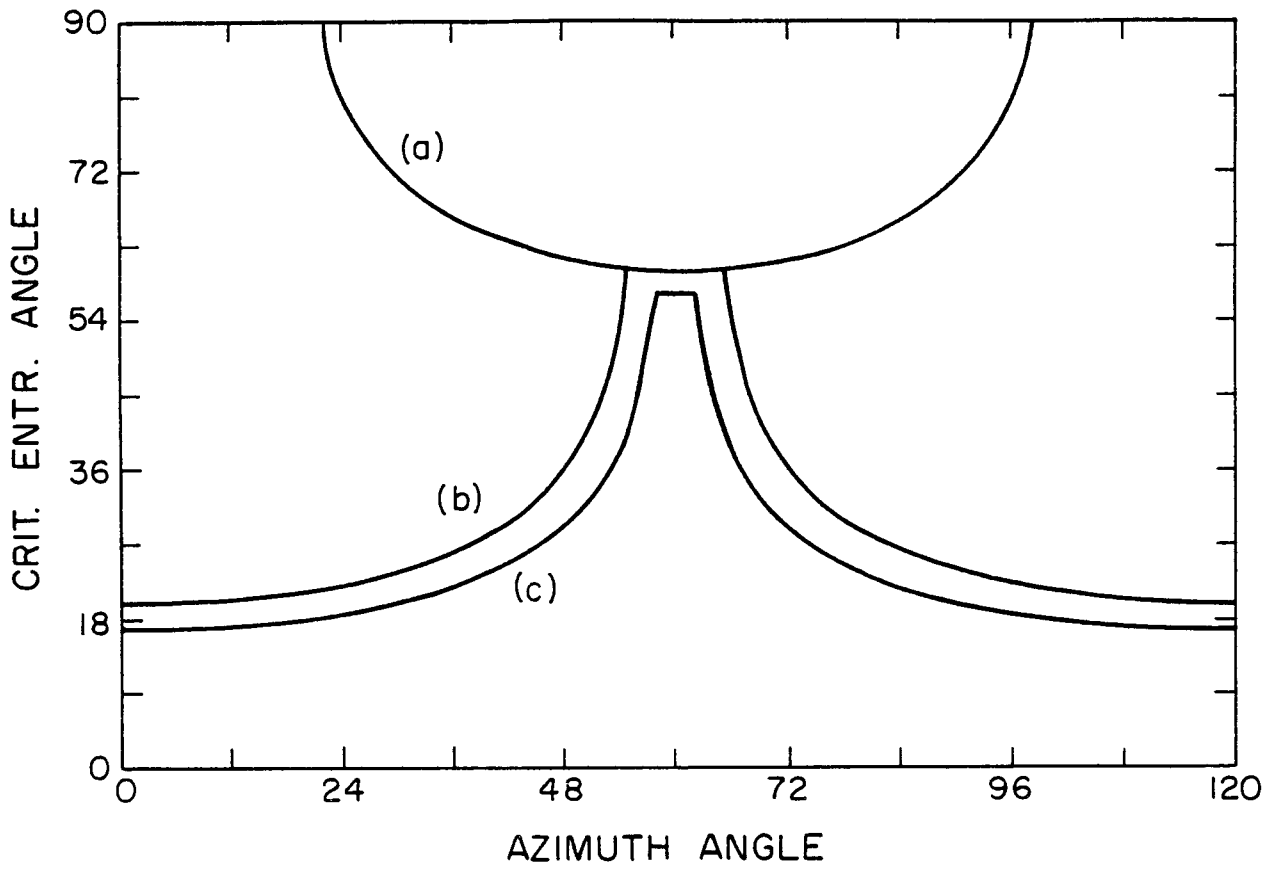

Figure 5. Variation of the maximum entrance angle under which the incident light is effectively or totally reflected at the triple-mirror system as a function of the azimuth angle γ. Line (a) and (b) represent these variations for the cases of the coated and uncoated triple-square-mirror systems, respectively, while line (c) represents that for the case of the uncoated triple-mirror system with a circular face.

If a CCR is tilted, the effective reflecting aperture has a symmetric streamlined shape as is shown unhatched in Fig. 1. Suppose the aperture is illuminated with a plane wave of the wave number k and the polarization represented by its electric field, $[E_{ix}, E_{iy}]^T e^{ik(z-ct)}$ where c is the velocity of light, and the superscript "T" refers to the transpose. We may choose E_{ix}, the x-component to be the TM component to the front window of the CCR, while E_{iy} to be TE component. Then, the far-field diffraction pattern of the retroreflected light may be found by the Fraunhoffer diffraction formula under the Kirchhoff's physical approximation. Considering the six different polarization outputs, one may express the electric field at the photodetector on the ground as $E_g(X,Y)e^{-ik(z+ct)}$ with the column vector,

$$E_g(X,Y) = \frac{k}{2\pi} \iint_{\text{aperture}} T_{out}\, M(\Theta)\, T_{in} \begin{bmatrix} E_{ix} \\ E_{iy} \end{bmatrix} \exp[-i \frac{k}{L} (Xx + Yy)]\, dxdy , \quad (13)$$

$$x = r \cos \Theta , \qquad y = r \sin \Theta , \quad (14)$$

aside from the constant phase factor. Here $i = \sqrt{-1}$, and L is the distance from the CCR to the receiver. (x,y) or (r,Θ) is the two-dimensional coordinate on the CCR aperture, while (X,Y) is that on the receiving plane. Note that the x-axis joins the center of the aperture and the center of the front window of the CCR on the projection plane. The origin on the (x,y) plane is chosen at the center of the effective reflecting aperture.

$$T_{in} = \begin{bmatrix} t_{TM}^{in} & 0 \\ 0 & t_{TE}^{in} \end{bmatrix} , \qquad T_{out} = \begin{bmatrix} t_{TM}^{out} & 0 \\ 0 & t_{TE}^{out} \end{bmatrix} . \quad (15)$$

Note that there are six different orders of reflection at the three corner mirrors, which gives the following six different matrix representations for the role of the triple corner-mirror system on polarization according to six different ranges of azimuth Θ.

$$M(\Theta) = \begin{cases} M_3\, M_2\, M_1\,, & \Theta_1 + \pi < \Theta \le M_3 \\ M_3\, M_1\, M_2\,, & \Theta_3 < \Theta \le \Theta_2 + \pi \\ M_1\, M_3\, M_2\,, & \Theta_2 + \pi < \Theta \le \Theta_1 \\ M_1\, M_2\, M_3\,, & \Theta_1 < \Theta \le \Theta_3 + \pi \\ M_2\, M_1\, M_3\,, & \Theta_3 + \pi < \Theta \le \Theta_2 \\ M_2\, M_3\, M_1\,, & \Theta_2 < \Theta \le \Theta_1 + \pi \end{cases} \tag{16}$$

$$M_j = R(-\Theta_j) \begin{bmatrix} \rho_{TM}(\psi_j) & 0 \\ 0 & \rho_{TE}(\psi_j) \end{bmatrix} R(\Theta_j), \qquad j = 1, 2, 3, \tag{17}$$

$$R(\Theta) = \begin{bmatrix} \cos\Theta & \sin\Theta \\ -\sin\Theta & \cos\Theta \end{bmatrix}, \tag{18}$$

$$\rho_{TM}(\psi_j) = - \frac{\cos\psi_j - i n \sqrt{n^2 \sin 2\psi_j - 1}}{\cos\psi_j + i n \sqrt{n^2 \sin^2\psi_j - 1}}, \tag{19}$$

$$\rho_{TE}(\psi_j) = \frac{n\cos\psi_j - i \sqrt{n^2 \sin^2\psi_j - 1}}{n\cos\psi_j + i \sqrt{n^2 \sin^2\psi_j - 1}}, \tag{20}$$

where the three angles of incidence to the three corner mirrors, ψ_1, ψ_2, and ψ_3, are given as their cosine values in Eqs.(5)-(7), respectively, while the angles α and β have been found in Eqs.(3)-(4). Various transmission coefficients in Eq.(14) are given in Eqs.(9)-(10). The six sectors of the

effective retroreflecting aperture are divided at $\Theta = \Theta_j$, $\Theta_j + \pi$, $j = 1, 2, 3$, whose tangents are given by (see Appendix D)

$$\tan\Theta_j = \tan\theta_j \, (\cos\phi/\cos\Phi), \quad j = 1, 2, 3 . \tag{21}$$

where Θ_j's are the azimuth angles dividing the six sectors viewed inside the CCR prism as shown in Fig. 6. They may be found from

$$\cos\Theta_1 = \frac{1 - \cos\alpha \cos\beta[\sin\alpha + \cos\alpha \, (\cos\beta + \sin\beta)]}{\sqrt{3} \sin\phi \sqrt{1 - \cos^2\alpha \cos^2\beta}} \tag{22}$$

$$\cos\Theta_2 = \frac{\sin^2\alpha - \sin\alpha \cos\alpha \sin\beta + \cos^2\alpha \cos\beta \, (\cos\beta - \sin\beta)}{\sqrt{3} \sin\phi \sqrt{1 - \cos^2\alpha \sin^2\beta}} \tag{23}$$

$$\cos\Theta_3 = \frac{\cos\alpha - \sin\alpha \, (\cos\beta + \sin\beta)}{\sqrt{3}\sin\phi} , \tag{24}$$

The ambiguity involved in the inverse trigonometry in Eq.(21) can be resolved by noting that the angles Θ_j and θ_j are in the same quadrant in the x-y plane.

The integration in Eq.(13) may be evaluated by the two-dimensional discrete Fourier transform. It may also be benefited by making use of the fact that the geometry has a radial symmetry.

In a special case of a CCR with the three corner mirrors that can preserve the polarization as in the case of highly reflecting metal-coated corner mirrors, $M_t(\Theta)$ can be considered as an identity matrix. In this case, the above integration (13) can be evaluated by the extended use of the two-dimensional Fourier transform of an isosceles and that of a trapezoid which were given in Ref.[7]. That is, we first segment the aperture into 2N stripes with an identical width as shown in Fig. 7. The two segments at the top and at

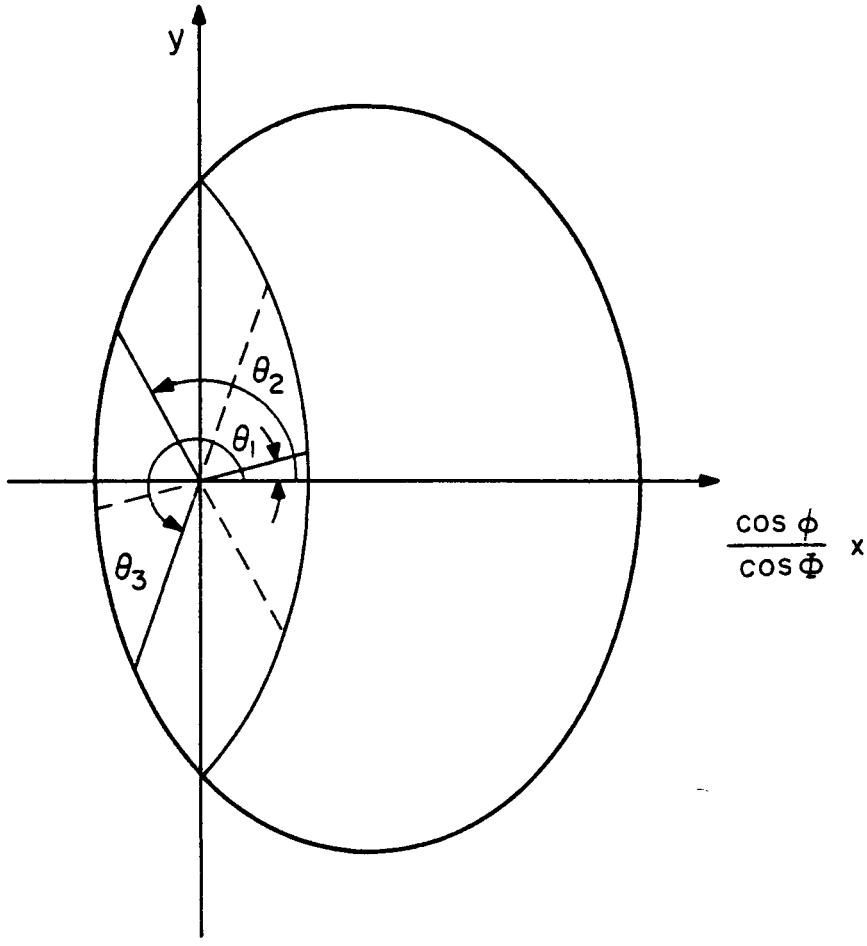

Figure 6. The front view of a cube-corner retroreflector seen inside along the internal axis ($\hat{\mathbf{p}}$) refracted from the external observation axis. The six sections are defined by the azimuths $\Theta = \Theta_m$, $\Theta_m + \pi$, $m = 1, 2, 3$.

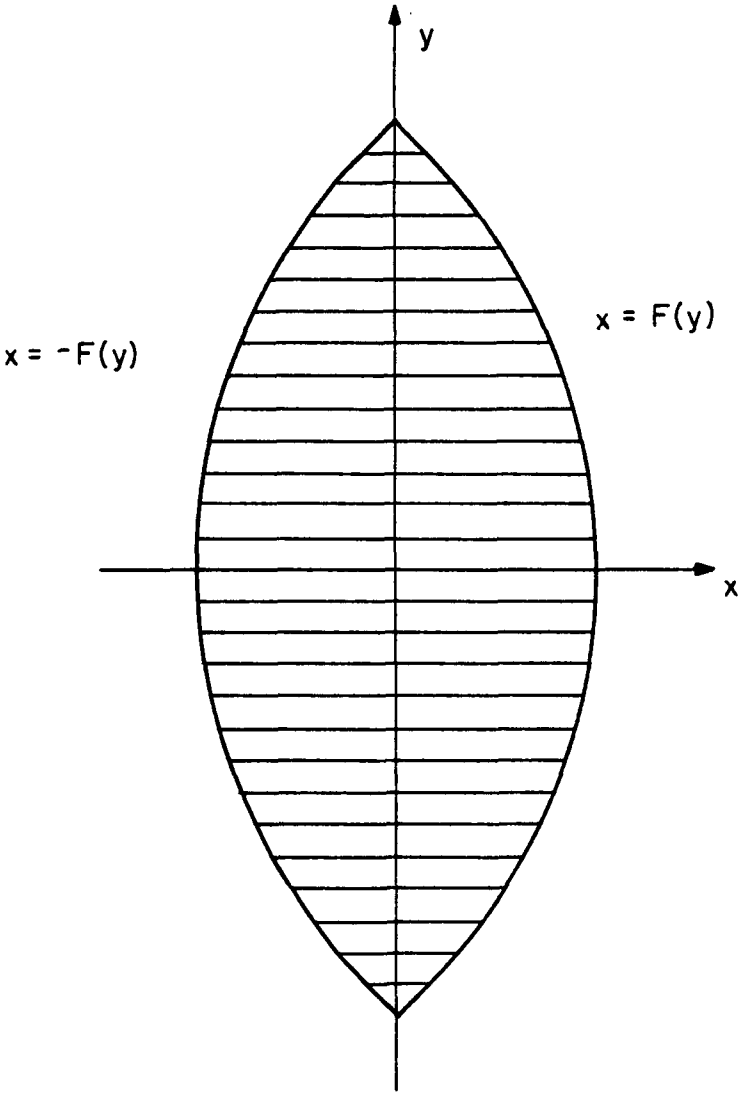

Figure 7. The streamline-shaped effective reflecting aperture is segmented into two isosceleses and a number of trapezoids symmetrically disposed with respect to the origin. Two outer lines are represented by $x = \pm F(y)$.

the bottom may be approximated into two isosceles located symmetrically with respect to the origin. All the other "2N-2" stripes may be approximated into trapezoids. They may be paired symmetrically with respect to the origin so that their superposed two-dimensional Fourier transform may be a real function on (X,Y). The two outer lines are represented by $x = \pm F(y)$, where

$$F(y) = \cos\Phi \, (\sqrt{1 - y^2} - \sqrt{2} \tan\phi). \tag{25}$$

Then the integration in (13) aside from premultiplying factors may be expressed as a superposition of I_n, $n = 1, \ldots, N$, each of which is the Fourier integral of a pair of trapezoids of an identical height h (an isosceles may be viewed as a trapezoid with a constricted upper latus).

$$\int_{-p}^{p} dy \int_{-F(y)}^{F(y)} dx \, \exp[-i(\xi x + \eta y)] = \sum_{n=1}^{N} I_n(\xi, \eta), \qquad \xi = \frac{kX}{L}, \; \eta = \frac{kY}{L}, \tag{26}$$

where $p = |F^{-1}(0)| = \sqrt{1 - 2\tan^2\phi}$, and $h = p/N$ in consequence

$$I_n(\xi, \eta) = \begin{cases} \frac{2h}{\xi} \{\sin(x_n\xi + y_n\eta) \, \mathrm{sink}[h(\eta + \alpha_n\xi)] \\ \quad + \sin(x_n\xi - y_n\eta) \, \mathrm{sink}[h(\eta - \alpha_n\xi)]\}, & \xi \neq 0 \\ 4h\{x_n \cos(yn\eta) \, \mathrm{sink}(h\eta) \\ \quad + \alpha_n y_n \mathrm{sink}(2y_n\eta) \, [(\cosh(\eta/2) - \mathrm{sink}(h\eta)]\}, & \xi = 0. \end{cases} \tag{27}$$

$$\mathrm{sink}\ \omega = \begin{cases} \frac{\sin(\omega/2)}{\omega/2}, & \omega \neq 0 \\ 1, & \omega = 0 \end{cases} \tag{28}$$

$$x_n = [F(nh) + F((n-1)h)]/2, \quad y_n = (n - 1/2)h \tag{29}$$

$$\alpha_n = [F(nh) - F((n-1)h)]/2 \ . \tag{30}$$

The FORTRAN program that computes Eqs.(26)-(30) was given in Appendix E, in which these equations were used for finding the lidar cross section of each CCR on the LAGEOS.

If a CCR is moving with the velocity component v′ which is perpendicular to the illumination axis, the Bradley or velocity aberration effect causes the reflected beam pattern to be angularly displaced by an amount [1]

$$\psi_v = 2v'/c \tag{31}$$

Here the aspect of CCR with respect to the illumination axis is relatively unchanged compared to the velocity of the CCR in moving. The lidar cross section is defined by [8]

$$\sigma = 4\pi \frac{\text{I(at the receiver)}}{\text{H(incident irradiance)}} \tag{32}$$

where H and I are the irradiances measured at the CCR and the receiver, respectively.

So far we have assumed that the CCR has no dihedral angle error and no other manufacturing errors. In fact, many CCRs have intentional dihedral angle errors so that the retroreflected beam may have a little degree of beam spread for practical purpose. The CCRs used in recent ranging satellites also have some degree of nominal dihedral angle error in the order of one arcsecond to have spreaded diffraction pattern at the receiver which is at the transmitter site [9].

The spread of the retroreflected beam induced by the dihedral angle error δ was found to be 3.26 $n\delta$, where n is the refractive index of the CCR prism [5]. More elaborate work to find the explicit expression for the six diverging reflected beams is found in Refs. [10] and [11]. The result of Chandler [11] can be incorporated into our analysis of the far field diffraction pattern.

Effects of some other manufacturing error which is random in nature was treated simply by supposing an equation of the form which provides the best fit to experimental datas [8].

IV. CONCLUSIONS

In this report, we have analyzed the lidar cross section of one CCR with either a circular front window or a hexagonal front window. Analytic expressions for the effective reflecting aperture of a CCR with a hexagonal window have been found. The polarization change as light is reflected and comes out is discussed with a CCR having either uncoated or coated corner mirrors. That change may be treated with the Jones calculus. The result of this report may directly be in use for CCR arrays either for traffic signs or for space use. The expression for the far-field diffraction pattern of a CCR has been obtained under the Kirchhoff's physical approximation on aperture diffraction, and analysis on the actual pattern to be obtained by the polarization analysis is reserved for future research. Besides analysis on the effect of the dihedral-angle error has not been included in this report. For an array of CCR, the intensity pattern in time for each CCR should be summed because of incoherency between reflections by individual CCRs. The far-field Fraunhoffer diffraction pattern will be useful in analyzing the lidar cross section of an array of CCRs in moving.

This work has been supported by NASA Goddard Space Flight Center.

APPENDIX A: DERIVATION OF EQUATIONS (3)-(4)

In Figure 2, the reference axis is represented by a unit vector, $\hat{c} = [1/\sqrt{3},\ 1/\sqrt{3},\ 1/\sqrt{3}]^T$, where the superscript "T" refers to the transpose. We shall denote by a unit vector $\hat{p}$ the direction of light being deflected from the illumination axis while entering the CCR window,

$$\hat{p} = [\cos\alpha \cos\beta,\ \cos\alpha \sin\beta,\ \sin\alpha]^T \tag{A.1}$$

Then from the cosine rule, $\hat{c} \cdot \hat{p} = \cos\phi$

$$\cos\phi = [\sin\alpha + \cos\alpha\ (\cos\beta + \sin\beta)]/\sqrt{3} \tag{A.2}$$

and from $|\hat{p} \times \hat{c}|\ \cos\gamma = \hat{p} \times \hat{c} \cdot [-1/\sqrt{2},\ 1/\sqrt{2},\ 0]^T$,

$$\tan\gamma = \frac{\sqrt{3}\ \cos\alpha\ (\cos\beta - \sin\beta)}{2\ \sin\alpha - \cos\alpha\ (\cos\beta + \sin\beta)} \tag{A.3}$$

From these two equations (A.2) and (A.3) we may find Eqs.(3)-(4).

APPENDIX B: DERIVATION OF EQUATION(12)

Assuming no dihedral angle error, one can see, including their images, three square mirrors each of which looks like bisecting the other two mirrors in the middle. The vertex of the CCR prism is at the center of each of the three square mirrors. Define a new two-dimensional Cartesian coordinate system for projection whose xy-plane is at right angle to the vector $\hat{\mathbf{p}}$ introduced in Appendix A. The vertex of the CCR prism is also chosen as the origin of the new coordinate system. One corner along the z-axis would lie on the x-axis on the plane of projection. One may assign four coordinates to four points of each of the three projected squares. It can be done systematically by the following matrix operation:

$$\begin{bmatrix} x \\ y \end{bmatrix} = \begin{bmatrix} 0 & 0 & 1 \\ 0 & 1 & 0 \end{bmatrix} R_Y(-\alpha') \, R_Z(\beta') \, \mathbf{a} \qquad \text{(B.1)}$$

where $\mathbf{a}$ is one of eight position vectors such as $[0\ 1\ 1]^T$, $[0\ 1\ -1]^T$, etc. R_Y and R_Z describe the passive rotations with respect to the y and z axes, respectively. Once all twelve projected coordinates are obtained, one can readily find the triply overlapped hexagon and find its area according to one of the four conditional phases of the hexagonal shape characterized by the corresponding four ranges of $\tan\alpha$ as were given in association with Eq.(12). Finally, considering the index difference, one should multiply it with $\cos\Phi/\cos\phi$.

APPENDIX C

```
>1.170P
      1:       NAME CCRPLT
      2: C-------------------------------------------------
      3: C   UPDATED ON FEB. 28, 1987   G. HUGH SONG
      4: C     makes a graph of the retro-reflectance
      5: C     as a function of the incidence angle DPHI
      6: C     with fixed values RI, DGAM, and DPOL.
      7: C
      8: C     RI: Refractive index of the CCR.
      9: C     CCR(DPHI): The resulting relative retro-reflectance normalized
     10: C           to the case of normal incidence
     11: C     REF  : retro-reflectance
     12: C     DGAM: See statement No. 302
     13: C     DPOL: See statement No. 308
     14: C
     15: C      This program assumes unpolarized input. Should be modified!
     16: C-------------------------------------------
     17:       DIMENSION RANGE(4),Y(180,1)
     18:       DIMENSION APHI(180),AREN(180),CCR(180)
     19:       DATA RANGE/180.,180.,0.,1.1/
     20:       RAD(DE)=DE*ATAN(1.)/45.
     21:       DEG(RA)=RA*45./ATAN(1.)
     22:       PI=4.*ATAN(1.)
     23: C-------------------------------------INPUT------------
     24:    1  WRITE(3,301)
     25:  301  FORMAT(/,/," ENTER THE FOLLOWING DATA >>>>",/,/,/,/,
     26:     +   " RI=REFRACTIVE INDEX OF THE CCR.",/,
     27:     +   "      (THAT OF FUSED SILICA IS 1.455)")
     28:       READ(3,*)RI
     29: C
     30:       WRITE(3,319)
     31:  319  FORMAT(///,
     32:     +" Is it an array of hexagonal CCRs (if so, type 1!),",//,
     33:     +" or a single CCR with a circular face (if so, type 0!) ?",//)
     34:       READ(3,*)LFACE
     35: C
     36:       WRITE(3,)"  NOW, IS THE CCR COATED?  YES-1, NO-0"
     37:   30  READ(3,)LCOAT
     38:       IF(LCOAT)30,2,31
     39:   31  WRITE(3,)"WE ASSUME THE METALLIC COAT IS A PERFECT REFLECTOR."
     40:    2  WRITE(3,302)
     41:  302  FORMAT(/," DGAM(deg)=ANGLE OF THE PLANE OF INCIDENCE",/,
     42:     +"   MEASURED FROM ONE EDGE DIRECTION (NORTH pole).",/,
     43:     +" 0. =< DGAM < 180.")
     44:       READ(3,)DGAM
     45:       GAM=RAD(DGAM)
     46: C
     47:       WRITE(3,306)
     48:  306  FORMAT(/,/," IS THE INCIDENT LIGHT POLARIZED?  YES-1, NO-0")
     49:  202  READ(3,) LPOL
     50:       IF(LPOL)202,204,203
     51: C
     52:  203  WRITE(3,308)
     53:  308  FORMAT(" Sorry. Not developed for polarized light."/,
     54:     +" The program assumes unpolarized light in the following.")
     55: C    +" WE SHALL ASSUME THAT THE LIGHT IS LINEARLY POLARIZED.",/,
     56: C    +" SPECIFY THE DIRECTION OF THE POLARIZATION IN deg,",/,
     57: C    +" so that DPOL=90. and DPOL=0. mean the TE and TM incidence."
     58: C    +,/," respectively.")
     59: C     READ(3,)DPOL
     60: C204  IF(LPOL.EQ.0) DPOL=45.
     61:  204  DPOL=45.
     62: C-----------------------------------------------
     63:       WRITE(3,307)
     64:  307  FORMAT(////," INCI.",T9,"Ref'ty",T20,"REF'ANCE",T40,"EFFECTIVE
     65:     +AREA",/," ANGLE",T40,"NORMALIZED",///)
     66: C
     67:       DO 81 I=1,180
     68:       APHI(I)=90.-FLOAT(I)
     69:       DPHI=ABS(APHI(I))
     70:       IF(I.EQ.90) GAM=GAM+PI
     71: C
     72:       CALL SUBCCR(RI,GAM,RAD(DPHI),LFACE,LCOAT,1,RAD(DPOL),ALP,
     73:     +BET,  DPHIM2,AREN(I),TRY,CCR(I),TOP)
```

```
C
      IF(I.EQ.2)DPHIM1=DPHIM2
      DALP=DEG(ALP)
      DBET=DEG(BET)
      WRITE(36,7)APHI(I),TRY,CCR(I),AREN(I),DALP,DBET,CCR(I)*AREN(I)
C     WRITE(3,7)APHI(I),TRY,CCR(I),AREN(I),DALP,DBET,CCR(I)*AREN(I)
 81   CONTINUE
 7    FORMAT(1X,F6.2,F10.6,T20,F10.6,T35,F10.6,2(2X,F8.3),2X,F10.6)
C
C------------------------------------ output and plot---
      WRITE(3,309)DGAM,DPHIM1,DPHIM2
 309  FORMAT(///,
     +"+    %%%%%%%%%%  EFFECTIVE REFLECTANCE OF CCR  %%%%%%%%%%",//,
     +//,' WHEN THE INCIDENCE PLANE (DGAM=',F10.6,'deg) IS FIXED.',/
     +//,' ACCEPTIBLE ANGLE OF INCIDENCE IS FROM',F9.6,' TO -',F9.6)
C
      WRITE(3,347)
 347  FORMAT(' WHICH TO PLOT? Type 1 for the beam relectivity CCR",/
     +      "                  OR Type 0 for the norm. eff. area AREN.")
      READ(3,) NY
      IF(NY.EQ.0)
       DO 83 I=1,180
 83     Y(I,1)=AREN(I)
       ELSE
       DO 84 I=1,180
 84     Y(I,1)=CCR(I)
       END IF
      CALL USPLO(APHI,Y,180,180,1,1,11HREFLECTANCE,
     +           11,5HANGLE,5,3HREF,3,RANGE,1H1,0,IER)
C-------------------------------------
      WRITE(3,)"DO YOU WANT TO RUN ONCE MORE? YES-1, NO-0."
      READ(3,)NY
      IF(NY.EQ.0) GO TO 997
 5    WRITE(3,) " With the same CCR? Yes-1, No-0"
      READ(3,) NY
      IF(NY) 5,1,2
C
 997  WRITE(3,)"WANT A PLOT ON THE ELEC. STATIC PLOTTER? Yes-1 No-0"
      READ (3,) NY
      IF(NY.EQ.1) CALL CCRGRM
 999  STOP
      END
C
C=============================================================
C
      SUBROUTINE CCRGRM
C           same as the PROGRAM CCRGRM.
      DIMENSION Y(180),RETNEAR(4,180),APHI(180),CCR(180),AREN(180)
      REWIND 36
      CALL PINIT(1.5, 5., 720)
      WRITE(3,21)
 21   FORMAT("How many sets of curves do you want to plot? (N<5)",/
     +," Each set = norm. eff. retroref. area & beam reflty."//,
     +" And you'll plot the near field ref'ance.",/)
      READ (3,) N
      WRITE(3,22)
 22   FORMAT(" 1st curve : thin solid      2nd : bold solid",/,
     +       " 3rd : thin dahed       4th : bold dahed.")
C
      DO 3 NPP=1,N
      DO 1 I=1,180
 1    READ(36,310)APHI(I),CCR(I),AREN(I),DALP,DBET,RETNEAR(NPP,I)
 310  FORMAT(1X,F6.2,T20,F10.6,T35,F10.6,2(2X,F8.3),2X,F10.6)
C
      IF(NPP.EQ.1)
       CALL MGRPHL(APHI,AREN,180,-90.,90., 0.,1., 6.,4.)
       CALL DATPL2(APHI,CCR,180,6,1,0,0.,6,1,6)
      ELSE IF((NPP.EQ.2).OR.(NPP.GT.4))
       CALL DATPL2(APHI,AREN,180,0,1,0,0.,0,4,0)
       CALL DATPL2(APHI,CCR,180,6,1,6,6.,6,4,6)
      ELSE IF(NPP.EQ.3)
       CALL DATPL2(APHI,AREN,180,0,1,0,0.,0,1,3)
       CALL DATPL2(APHI,CCR,180,0,1,0,0.,0,1,3)
      ELSE IF(NPP.EQ.4)
```

```
>148,180P
   148:           CALL DATPL2(APHI,AREN,180,0,1,0,0.,  0,4,3)
   149:           CALL DATPL2(APHI,CCR,180,0,1,0,0.,  0,4,3)
   150:         END IF
   151:    3    CONTINUE
   152:   C
   153:         CALL TITLE(1HB,21HINCIDENCE ANGLE (deg),21,.14,1)
   154:         CALL WHERE
   155:   C
   156:         CALL PINIT(1.5, 5., 720)
   157:         DO 4,NPP=1,N
   158:         DO 5 I=1,180
   159:    5    Y(I)=RETNEAR(NPP,I)
   160:         IF(NPP.EQ.1) CALL MGRPHL(APHI,Y,180,-90.,90.,0.,1.,6.,4.)
   161:         IF(NPP.EQ.2) CALL DATPL2(APHI,Y,180,0,1,0,0.,0,4,0)
   162:         IF(NPP.EQ.3) CALL DATPL2(APHI,Y,180,0,1,0,0.,0,1,3)
   163:         IF(NPP.EQ.4) CALL DATPL2(APHI,Y,180,0,1,0,0.,0,4,3)
   164:    4    CONTINUE
   165:         CALL TITLE(1HL,27HNEAR FIELD RETROREFLECTANCE,27,.14,1)
   166:         CALL TITLE(1HB,21HINCIDENCE ANGLE (deg),21,.14,1)
   167:         CALL WHERE
   168:         RETURN
   169:         END
   170:   C
   171:   C=================================================================
   172:   C
   173:         SUBROUTINE SUBCCR(RI,GAM,PHI,LFACE,LCOAT,LFRESN,POL,
   174:        + ALP,BET,   DPHIM,ARN,REF,REFFR,TOP)
   175:   C
   176:   C                              G. HUGH SONG, FEB. 21, 1987
   177:   C
   178:   C      COMPUTES THE REFLECTANCE OF A CUBE CORNER RETROREFLECTOR
   179:   C      FROM SPECIFIED DATA OF THE RI, GAM, PHI ANGLES.
   180:   C
```

```
>1,92F:       PROGRAM CRITANG
    2:  C-------------------------------------------------------
    3:  C    UPDATED ON NOV. 12, 1986   G. HUGH SONG
    4:  C      outputs the critical entrance angle
    5:  C      that depends on the azimuth angle DGAM
    6:  C      with fixed values RI and DPOL.
    7:  C
    8:  C      RI: Refractive index of the CCR.
    9:  C      CCR(DPHI): The resulting relative retro-reflectance normalized
   10:  C            to the case of normal incidence
   11:  C      REF : retro-reflectance
   12:  C      DGAM: See statement No. 302
   13:  C      DPOL: See statement No. 308
   14:  C
   15:  C     SUBROUTINE : SUBCCR
   16:  C
   17:  C-----------------------------------------
   18:        RAD(DE)=DE*ATAN(1.)/45.
   19:        DEG(RA)=RA*45./ATAN(1.)
   20:        PI=4.*ATAN(1.)
   21:  C-----------------------------------INPUT------------
   22:    1   WRITE(3,301)
   23:    301 FORMAT(/,/," ENTER THE FOLLOWING DATA >>>>",/,/,/,/,
   24:       +  " RI=REFRACTIVE INDEX OF THE CCR.",/,
   25:       +  "      (THAT OF FUSED SILICA IS 1.455)")
   26:        READ(3,*)RI
   27:  C
   28:        WRITE(3,319)
   29:    319 FORMAT(///,
   30:       +" Is it an array of hexagonal CCRs (if so, type 1!),",//,
   31:       +" or a single CCR with a circular face (if so, type 0!) ?",//)
   32:        READ(3,*)LFACE
   33:  C
   34:        WRITE(3,)"  NOW, IS THE CCR COATED?  YES-1, NO-0"
   35:    30  READ(3,)LCOAT
   36:        IF(LCOAT)30,32,31
   37:    31  WRITE(3,)"WE ASSUME THE METALLIC COAT IS A PERFECT REFLECTOR."
   38:        GO TO 201
   39:  C-----------------------------------
   40:    32  WRITE(3,311)
   41:    311 FORMAT(" When the condition of total reflection is not ",/,
   42:       +" satisfied inside the CCR, we ignore the reflectance",/)
   43:  C
   44:    201 WRITE(3,306)
   45:    306 FORMAT(/,/," IS THE INCIDENT LIGHT POLARIZED?  YES-1, NO-0")
   46:    202 READ(3,) LPOL
   47:        IF(LPOL)202,204,203
   48:  C
   49:    203 WRITE(3,308)
   50:    308 FORMAT(/,
   51:       +" WE SHALL ASSUME THAT THE LIGHT IS LINEARLY POLARIZED.",/,
   52:       +" SPECIFY THE DIRECTION OF THE POLARIZATION IN deg,",/,
   53:       +" so that DPOL=90. and DPOL=0. mean the TE and TM incidence,"
   54:       +,/," respectively.")
   55:        READ(3,)DPOL
   56:  C-------------------------------------------------
   57:    204 WRITE(3,307)
   58:    307 FORMAT(////," AZIMUTH ",T20,"CRITICAL ANGLE",T40,"EFFECTIVE
   59:       +AREA",///)
   60:  C
   61:        DO 81 IG=0,120       ! FORTRAN 77
   62:        DGAM=FLOAT(IG)
   63:        GAM=RAD(DGAM)
   64:        DELT=45.
   65:        DPHI=45.
   66:    41  CALL SUBCCR(RI,GAM,RAD(DPHI),LFACE,LCOAT,0,POL,ALP,
   67:       +BET,  DPHIM2,AREN,TOTREF,REF,TOP)
   68:        CCR=AREN*AREN*REF  ! Fraunhoffer diffraction.
   69:        IF(REF.GT.0.) DELT=ABS(DELT/2.)
   70:        IF(REF.LE.0.) DELT=-ABS(DELT/2.)
   71:        DPHI=DPHI+DELT
   72:        IF(ABS(DELT).GT.1.E-3)GO TO 41
   73:  C
```

```
      DALP=DEG(ALP)
      DBET=DEG(BET)
      WRITE(36,310)DGAM,AREN,DPHI,DALP,DBET
   81 WRITE(3,310) DGAM,AREN,DPHI,DALP,DBET
  310 FORMAT(1X,F6.2,T20,F10.6,T40,F10.6,2(2X,F8.3))
C-----------------------------------
      WRITE(3,)"DO YOU WANT TO RUN ONCE MORE? YES-1, NO-0."
      READ(3,)NY
      IF(NY)999,999,1
  999 STOP
      END
C
C=============================================================
C
      SUBROUTINE SUBCCR(RI,GAM,PHI,LFACE,LCOAT,LFRESN,POL,
     + ALP,BET,   DPHIM,ARN,REF,REFFR,TOP)
C
C                              G. HUGH SONG, FEB. 21, 1987
C
```

```
>1,>P
      PROGRAM CRITGRM
      DIMENSION X(0:120),Y(0:120),DGAM(0:120),CRIT(0:120)
      CALL PINIT(1.5, 5., 600)
      N=0
C
    3 DO 1 I=0,120
      READ(36,310)DGAM(I),SOMETH,CRIT(I)
    1 CONTINUE
  310 FORMAT(1X,F6.2,T20,F10.6,T40,F10.6,2(2X,F8.3))
C
      DO 2 I=0,120
      X(I)=DGAM(I)
      Y(I)=CRIT(I)
    2 CONTINUE
      IF(N.EQ.0)
      CALL MGRPHL(X,Y,121, 0.,120., 0.,90., 6., 4.)
       ELSE
       CALL DATPL2(X,Y,121, 0,1,0,0., 0, 3, 0)
      END IF
      N=N+1
      IF(N.LT.3) GO TO 3
C
      CALL TITLE(1HL,17HCRIT. ENTR. ANGLE, 17, .14, 1)
      CALL TITLE(1HB,13HAZIMUTH ANGLE,13, .14, 1)
      CALL WHERE
      STOP
      END
```

APPENDIX D: DERIVATION OF EQUATIONS (21)-(24)

For the moment, we suppose a CCR with unit refractive index. Then we can see a tilted front view of a CCR along the observation axis which is the illumination axis at the same time. Then we then have the six sectors and six angles Θ_1, $\Theta_3 + \pi$, Θ_2 $\Theta_1 + \pi$, Θ_3, and $\Theta_1 + \pi$ that define the six sectors as shown in Fig. 5. Using the cosine rule, we can find the cosine of Θ_1, Θ_2, and Θ_3 as

$$\cos\Theta_j = \frac{\hat{c} \times \hat{p} \cdot \hat{e}_j \times \hat{p}}{|\hat{c} \times \hat{p}||\hat{e}_j \times \hat{p}|} , \qquad j = 1, 2, 3 , \tag{D.1}$$

which will give Eqs.(21)-(23). Here $\hat{e}_1$, $\hat{e}_2$, and $\hat{e}_3$ are the unit vectors directing along the three corners inside a CCR.

Next, for a CCR with the refractive index n, those Θ_j's will appear at Θ_j in the ellipce whose short axis is the more shortened by the ratio $\cos\Phi/\cos\phi$ while the long axis remains the same. Therefore Θ_j and Θ_j are related by Eq.(21).

APPENDIX E

```
>1,71P
      1:       NAME DIFPAT
      2: C.....................................
      3: C                      G.HUGH SONG , updated on APRIL 15, 1986
      4: C     gives the diffraction pattern for a symmetric pupil function
      5: C     F(y), which is givn in a function subprogram
      6: C-------------------------------------------------------------
      7:       DOUBLE PRECISION*6 TOP
      8:       DIMENSION RANGE(4),SPFR(100),A(100,1)
      9:       COMMON /COMF/PHI,TAP
     10:       CHARACTER*1 XORY
     11:       DATA RI/1.455/,RANGE/0.,0.,0.,0./
     12:       RAD(DEG)=DEG*ATAN(1.)/45.
     13: C.....................................
     14:  9    WRITE(3,)"INPUT DPHI IN deg!   DPHI="
     15:       READ(3,)DPHI
     16:       PHI=RAD(DPHI)
     17:       SIP=SIN(PHI)/RI
     18:       TAP=SIP/SQRT(1.-SIP*SIP)
     19:       TOP=SQRT(1.-2.*TAP*TAP)
     20:       WRITE(3,)" HOW MANY STRIPES DO YOU TAKE FROM ZERO TO TOP?"
     21:       READ(3,)M
     22: C
     23:  10   WRITE(3,)"WHICH SP. FREQ. COORD. DO YOU WANT TO FIX, X OR Y?"
     24:       WRITE(3,)"TYPE 'X' FOR X, OR 'Y' FOR Y WITH THE QUOT. MARKS!"
     25:       READ(3,)XORY
     26:       WRITE(3,)"SET VALUE FOR THAT SP.COORD.!"
     27:       READ(3,)FRFIX
     28:       IF(XORY.EQ.'X')
     29:         X=FRFIX
     30:         ELSE
     31:         Y=FRFIX
     32:        END IF
     33:  11   WRITE(3,)"TO WHAT SP. FREQ. FROM ZERO DO YOU WANT TO PLOT?"
     34:       READ(3,) FRMAX
     35:       DF=FRMAX/100.
     36: C
     37:       DO 100 I=1,100
     38:       SPFR(I)=(I-1)*DF
     39:       IF(XORY.EQ.'X')
     40:         Y=SPFR(I)
     41:         ELSE
     42:         X=SPFR(I)
     43:        END IF
     44:  100  CALL FT2D(X,Y,M,TOP,A(I,1))
     45:       WRITE(3,101)M,TOP,XORY,XORY,FRFIX
     46:  101  FORMAT(//," NO. OF SEGMENTED TRAPEZOIDS,",T40,"M=",I4,/,
     47:      +" THE PUPIL FUNCTION IS SPREAD IN",T40,"Y = +-",G10.3,/,
     48:      +" THE ",A1,"-SPAT. FREQ. IS FIXED AT ",A1," =",G10.3)
     49:       CALL USPLO(SPFR,A,100,100,1,1,13H2D FOURIER TR,13,
     50:      +          10HSPATIAL FR,10,2HFT,2,RANGE,1H1,0,IER)
     51:       WRITE(3,)
     52:      +"DO YOU WANT TO PLOT WITH A DIFFERENT SCALE? YES-1, NO-0"
     53:       READ(3,) NY
     54:       IF(NY.EQ.1)GO TO 11
     55:       WRITE(3,120)XORY,FRFIX
     56:  120  FORMAT(///," YOU HAVE BEEN SETTING ",A1,"=",G10.3,"SO FAR.",/,
     57:      +" DO YOU WANT TO PLOT WITH A DIFFERENT SETTING? YES-1, NO-0",)
     58:       READ(3,)NY
     59:       IF(NY.EQ.1)GO TO 10
     60:       WRITE(3,)
     61:      +" DO YOU WANT TO ANALYZE THE SHAPE WITH A DIFFERENT DPHI?"
     62:       READ(3,)NY
     63:       IF(NY.EQ.1)GO TO 9
     64:       STOP
     65:       END
     66: C
     67: C=============================================================
     68: C
     69:       SUBROUTINE FT2D(X,Y,M,TOP,AFT)
     70: C.....................................
     71: C              G. HUGH SONG, updated on APRIL 17, 1986
```

REFERENCES

1. P. O. Minot, Design of Retroreflector Arrays for Laser Ranging of Satellites, NASA Tech. Report X-723-74-122, March 1974.
2. R. F. Chang, D. G. Currie, C. O. Alley, and M. E. Pittman, "Far-field diffraction pattern for corner reflectors with complex reflection coefficients," J. Opt. Soc. Am., 61, No. 4, 431-438, April 1971.
3. M. Born and E. Wolf, Principles of Optics, 6th ed., Pergamon, Oxford, 1980.
4. G. H. Song and S. S. Choi, "Analysis of birefringence in single-mode fibers and theory for the backscattering measurement," J. Opt. Soc. Am. A., 2, No. 2, 167-170, February 1985.
5. R. C. Spencer, Optical Theory of the Corner Reflector, MIT Radiation Lab Rep. 433, March 1944.
6. H. D. Eckardt, "Simple model of corner reflector phenomena," Appl. Opt., 10, No. 7, July 1971. Also see H. D. Eckardt, "Correction to: Simple model of corner reflector phenomena," Appl. Opt., 10, No. 11, November 1971.
7. R. C. Smith and J. S. Marsh, "Diffraction patterns of simple apertures," J. Opt. Soc. Am., 64, No. 6, 798-803, June 1974.
8. P. O. Minot, Measurements of the Lidar Cross Sections of Cube Corner Arrays for Laser Ranging of Satellites, NASA Tech. Rep. X-722-74-301, Goddard Space Flight Center, Greenbelt, Maryland, September 1974.
9. J. L. Zurasky, "Cube corner retroreflector test and analysis," Appl. Opt., 15, No. 1, 445-452, February 1976.
10. P. Yoder, Jr., "Study of light deviation errors in triple mirrors and tetrahedral prisms," J. Opt. Soc. Am., 48, 496-499, 1958.

11. K. N. Chandler, "On the effects of small errors in the angles of corner-cube reflectors," J. Opt. Soc. Am., 50, 203-206, March 1960.

PART II. ERROR ESTIMATION OF SINGLE-COLOR LASER RANGING WITH A CUBE-CORNER-RETROREFLECTOR ARRAY AND ITS APPLICATION TO LAGEOS

ABSTRACT

The performance of a correlation estimator for the single-color laser ranging with a cube-corner retroreflector-array satellite as the ranging target is analyzed. The pulse shape of the laser source and the impulse response of the photodetector being considered as Gaussian shape, pulse broadening by split reflections at the array of cube-corner retroreflectors is analyzed. In this case of Gaussian approximations on the source and the detector, an expression for the root-mean-square of the timing error in ranging has been obtained under the assumption that shot noise and speckle-induced noise are not severe. Such analysis has been applied to a simulated ranging experiment with an existing satellite LAGEOS having 426 cube-corner retroreflectors to estimate the lower bound for the variance of the timing error.

I. INTRODUCTION

An array of cube-corner-retroreflectors (CCRs) has been used as a target for laser ranging. It may be employed in land surveying. It has long been used in satellite ranging in the National Aeronautics and Space Administration (NASA) [1]. By measuring the roundtrip time of pulsed laser light, we can estimate the distance from the ground station to the target. Among various methods for detection and estimation of received light signal, the correlation algorithm [2] is studied for ranging in this report. The correlation estimation technique has several advantages over other techniques. That considers both the shot noise and time-resolved speckle. It does not introduce a signal dependent bias that appears in the leading edge threshold technique [3]. It is optimum even for non-Gaussian pulses. All current laser ranging systems use one wavelength (single-color) of laser light. Hence analysis on single-color ranging is more needed than that on two-color ranging. In fact, the correlation algorithm for single-color ranging is simpler to analyze than that for two-color ranging.

In this report, explicit formulas are presented for single-color ranging with the target having an array of identical CCRs whose scattering cross sections may vary according to their locations on the target. The algorithm is then applied to a simulated ranging experiment with the Laser Geodynamic Satellite (LAGEOS). This satellite plays a key role in NASA's Earth and Ocean Dynamics Application Program [1]. It was designed as a passive long-lived target with a stable well-defined orbit. It has 426 CCRs of a circular-front-face type, so that laser light may be reflected and returned to the ground-based station. Variation of the scattering cross section according to the location on the LAGEOS has been studied. The root-mean-square (RMS) of the

ranging time error is calculated analytically and discussed with some exemplary situations of the LAGEOS.

II. THE CORRELATION ALGORITHM FOR SINGLE-COLOR RANGING WITH AN ARRAY OF CUBE CORNER RETROREFLECTORS

The pulsed laser light beam is assumed to have a sufficient beamwidth and a homogeneous wavefront over the surface of the target when it reaches the target surface. In this incidence we shall consider the signal amplitude at a certain point on the target, e.g., the point nearest to the light source, as a sequence of pulses. Individual pulses are well separated in time from each other and the RMS amplitude of those pulses is normalized and represented by f(t). After the light is reflected at each CCR, it is subject to diffraction. In addition, the signal power P(t) being detected at the receiver has uncertainty since the light components reflected at different CCRs have certain path differences between those components and therefore interfere with each other unless the individual pulse is short enough to resolve all CCRs spatially. We assume that the CCR array changes its aspect with respect to the observer slowly, but fast enough to cancel the net interference effect in the long run. The power averaged over such random phases can be expressed as

$$\langle P(t) \rangle = A \sum_{m=1}^{M} \sigma_m |f(t - \Psi_m)|^2 \qquad (1)$$

without any cross terms. Here A is a proper proportional constant. The summation is taken over all CCRs that have nonzero lidar cross sections σ_m. Ψ_m is the time dilation associated with the reflection at the mth CCR. Taking an average over the random phase, one may express the covariance of P(t) as

$$C_P(t_1,t_2) = A^2 \sum_{\substack{m \\ m\neq n}}^{M} \sum_{n}^{M} \sigma_m \sigma_n f(t_1 - \Psi_m)\, f^*(t_1 - \Psi_n)\, f(t_2 - \Psi_m)\, f^*(t_2 - \Psi_n), \tag{2}$$

where the asterisk refers to complex conjugation. The signal-to-noise ratio (SNR) is then defined as

$$R_{SN} = \left[\int_{-\infty}^{\infty} \langle P(t)\rangle dt\right]^2 \Big/ \iint_{-\infty}^{\infty} C_P(t_1,t_2)\, dt_1 dt_2 \tag{3}$$

In the case of direct detection, the mean and the autocovariance of the signal at the photon counter output become, according to the Campbell's theorem [4],

$$\langle S(t)\rangle = \frac{\eta}{h\omega} \langle P(t)\rangle * h(t)\ , \tag{4}$$

$$C_s(t_1,t_2) = \frac{\eta}{h\omega} \int_{-\infty}^{\infty} P(\tau)\, h(t_1-\tau)\, h(t_2-\tau)\, d\tau$$

$$+ \left(\frac{\eta}{h\omega}\right)^2 \int_{-\infty}^{\infty} \int_{-\infty}^{\infty} C_p(\tau_1,\tau_2)\, h(t_1-\tau_1)\, h(t_2-\tau_2)\, d\tau_1\, d\tau_2\ , \tag{5}$$

where η is the efficiency of the photodetector and $h\omega$ is the energy of a single photon. $h(t)$ is the normalized photodetector-impulse-response which may be approximated as a Gaussian function, $G(\sigma_h, t)$, with a RMS pulsewidth, σ_h, where

$$G(\sigma,\ t) = \frac{1}{\sqrt{2\pi}\ \sigma} \exp\left(-\frac{t^2}{2\sigma^2}\right) \tag{6}$$

If we also approximate the transmitted pulse intensity as another Gaussian function, i.e., $|f(t)|^2 = G(\sigma_f, t)$, then $\langle S(t)\rangle$ and $C_s(t_1, t_2)$ in Eqs.(4) and (5) become [5]

$$\langle S(t)\rangle = \langle N\rangle f_s(t, \sigma_g) , \tag{7}$$

$$C_s(t_1, t_2) = \langle N\rangle G(\sqrt{2}\sigma_h, t_1-t_2) f_s(\frac{t_1+t_2}{2}, \sigma_s) + \frac{\langle N\rangle^2}{R_{SN}} G(\sqrt{2}\sigma_g, t_1-t_2) f_{sp}(\frac{t_1+t_2}{2}), \tag{8}$$

where $\langle N\rangle$ is the average number of detected photons per pulse, and

$$\sigma_g = \sqrt{\sigma_f^2 + \sigma_h^2}, \qquad \sigma_s = \sqrt{\sigma_f^2 + \sigma_h^2/2}, \tag{9}$$

$$f_s(t, \sigma) = \sum_{m=1}^{M} \sigma_m G(\sigma, t-\Psi_m) \Big/ \sum_{m=1}^{M} \sigma_m , \tag{10}$$

$$f_{sp}(t) = \frac{\sum_{m=1}^{M}\sum_{\substack{n=1 \\ m\neq n}}^{M} \sigma_m \sigma_n \exp\left[-\frac{(\Psi_m-\Psi_n)^2}{4\sigma_f^2}\right] G(\frac{\sigma_g}{\sqrt{2}}, t - \frac{\Psi_m+\Psi_n}{2})}{\sum_{m=1}^{M}\sum_{\substack{n=1 \\ m\neq n}}^{M} \sigma_m \sigma_n \exp\left[-\frac{(\Psi_m-\Psi_n)^2}{4\sigma_f^2}\right]} . \tag{11}$$

According to Eq.(3), the SNR is found for a uniformly illuminated array of CCRs

$$R_{SN} = \Big(\sum_{m=1}^{M} \sigma_m\Big)^2 \Big/ \sum_{\substack{m\,n \\ m\neq n}}^{M\,M} \sigma_m\,\sigma_n \exp\Big[-\frac{(\Psi_m-\Psi_n)^2}{4\sigma_f^2}\Big] \,. \qquad (12)$$

A correlation estimator is used to determine the arrival time of the reflected signal. A schematic diagram is depicted in Fig. 1 to describe the principle of the correlation estimator for single-color ranging. A laser pulse with the pulsewidth σ_f (assumed to be a non-random variable) deflected by a beam splitter is detected at the detector D_1 directly at the ground station. The width and timing of the laser pulse may be measured at this stage. Here most of the pulsed laser power is directed to the target (LAGEOS). Being reflected at the target, the light returns to the ground station and is detected at the detector D_2. The pulsewidths of both detectors' impulse responses are the same, and are σ_h. Let τ be the random variable representing the time elapsed until the pulse returns from the target. Then τ is to be measured from the two outputs of the detectors D_1 and D_2. These output signals are supposed to be processed with infinite speed for correlation.

Each output signal S(t) at D_2 may be quite different from the previous ones since the target changes its aspect with respect to the light source even though the aspect is very slowly changing. This continuous change of S(t) is due to speckle. The speckle-induced noise can change the detected signal pattern because individual light pulses reflected at different CCRs interfere with each other unless light pulses are narrow enough to resolve individual CCRs.

Now we shall suppose an expected received signal $\bar{S}(t)$ by simulation as if

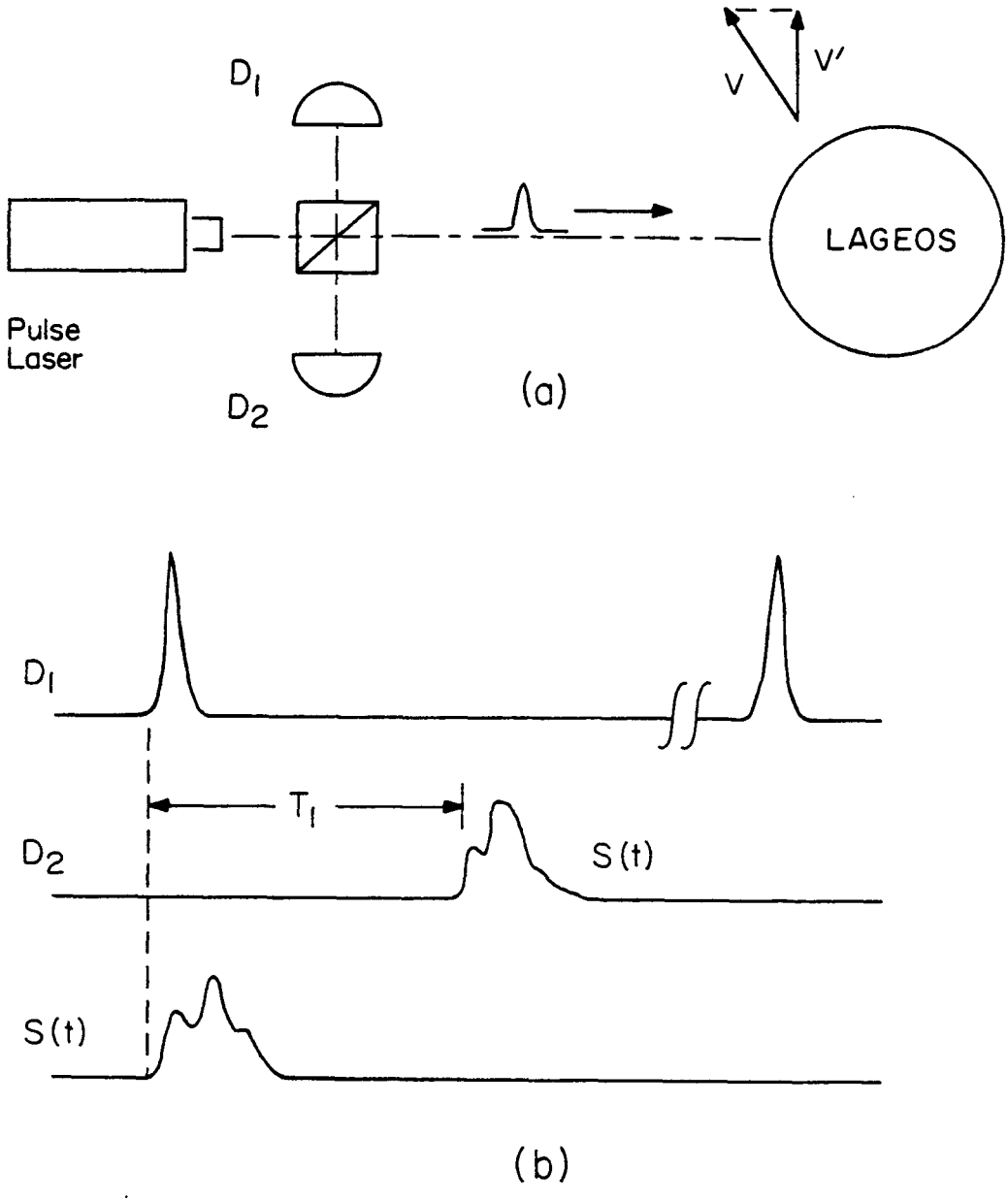

Figure 1. (a) Schematic diagram of the single-color laser ranging system with LAGEOS as the ranging target. (b) Pulse patterns at the output of the photodetectors D_1 and D_2 with a Gaussian-shaped impulse response (FWHP = $2\sigma_h$) and a Gaussian-shaped pulse laser having FWHP = $2\sigma_f$. In the same time scale the expected pattern S(t) is also illustrated. See text for details.

the LAGEOS were laid right behind the beam splitter and illuminated by a uniform plane wave. We then correlate S(t) with the actual received signal $\bar{S}(t)$ as

$$R(\tau) = \int_{-\infty}^{\infty} \bar{S}(t-\tau)\, S(t)\, dt \ . \tag{13}$$

This is the cross correlation function of the two signals when S(t) is assumed to be stationary. Here we assume that, compared to the motion of the target, the repetition rate of the light pulse source is so high that we may neglect the change of the aspect of the target with respect to the observing station. Still, it is assumed that the slight change of path-length difference of light components reflected at different CCRs gives rise to totally random phase-difference between those light components. In this respect, we can use the expectation as the average over the random phase. Also we assume that there exists an accurate delay to locate the expected signal $\bar{S}(t-\tau)$ when correlating. Then the correlation estimator can be written mathematically as

$$\tau_{COR} = \arg[\max_{\tau} R(\tau)] \ . \tag{14}$$

Using a Taylor-series expansion [6], we linearize $dR(\tau)/dt$ around $\tau = \tau_r$, the representative round-trip time obtained by astronomical computation or by averaging past several τ_{COR}'s.

$$\frac{d}{dt} R(\tau) \tilde{=} \frac{d}{d\tau} R(\tau)\Big|_{\tau_r} + (\tau-\tau_r) \frac{d^2}{d\tau^2} R(\tau)\Big|_{\tau_r} \ . \tag{15}$$

$dR(\tau)/d\rho$ vanishes at $\tau = \tau_{COR}$ where $R(\tau)$ is maximum. Therefore

$$\tau_{COR} \tilde{=} \tau_r - \frac{dR(\tau)}{d\tau}\Big|_{\tau_r} \Big/ \frac{d^2R(\tau)}{d\tau^2}\Big|_{\tau_r} , \tag{16}$$

provided that $d^2R(\tau)/d\tau^2$ does not vanish at $\tau = \tau_r$. This gives the newly measured τ_{COR}. Note that the validity of Eq.(16) strongly depends on the validity of Eq.(15). So when the detector output has rugged peaks due to split reflections at CCRs, we should obtain τ_{COR} by choosing the maximum among several peaks of $R(\tau)$ according to Eq.(14).

To evaluate the performance of the correlation estimator, we shall consider the mean square error of τ_{COR} when τ_r is ideally chosen at τ_o, the true round trip time. Under the assumption that the shot noise and the speckle are not so severe that

$$\mathrm{var}\left(\frac{d^2R(\tau)}{d\tau^2}\Big|_{\tau_o}\right) << \left\langle \frac{d^2R(\tau)}{d\tau^2}\Big|_{\tau_o} \right\rangle^2 , \tag{17}$$

the variance of τ_{COR}, $\langle \Delta\tau_{COR}{}^2 \rangle$ of the correlation estimator, defined as

$$\langle \Delta\tau_{COR}{}^2 \rangle = \langle (\tau_{COR} - \langle \tau_{COR} \rangle)^2 \rangle , \tag{18}$$

can be calculated. Now we shall assume that by monitoring the LAGEOS we have the complete information on the aspect of the LAGEOS - the information on which face directs the ground station with what azimuth angle. Then, since both the speckle and the shot noise induced fluctuations in one shot of detected pulse is uncorrelated with those of previous pulses, we may assume that supposed expected detected signal may have the structural peaks due to timely resolved CCRs and that $\bar{S}(t - \tau_o)$ is equal to $\langle S(t) \rangle$. Therefore

$$\frac{\partial}{\partial\tau}\bar{S}(t-\tau)\Big|_{\tau_o} = -\frac{\partial}{\partial t}\bar{S}(t-\tau_o) = -\frac{d}{dt}\langle S(t)\rangle \ . \tag{19}$$

This enables us to express the bias $\langle\tau_{COR}\rangle - \tau_o$ of the correlation estimator in terms of the mean function of S(t)

$$\langle\tau_{COR}\rangle - \tau_o = \int_{-\infty}^{\infty}\langle S(t)\rangle\frac{d}{dt}\langle S(t)\rangle dt \Big/ \int_{-\infty}^{\infty}\langle S(t)\rangle\frac{d^2}{dt^2}\langle S(t)\rangle dt \ . \tag{20}$$

As long as $\langle S(t)\rangle$ is a normalizable function, the denominator vanishes. Consequently, $\langle\tau_{COR}\rangle = \tau_o$. This result is quite reasonable since τ_o is the true round trip time. The same reasoning applies to derivation of the expression for $\langle\Delta\tau_{COR}{}^2\rangle$.

$$\langle\Delta\tau_{COR}{}^2\rangle = \langle(\tau_{COR} - \tau_o)^2\rangle \tilde{=} \left\langle\left[\frac{dR(\tau)}{d\tau}\right]^2_{\tau_o}\right\rangle \Big/ \left\langle\frac{d^2R(\tau)}{d\tau^2}\Big|_{\tau_o}\right\rangle^2$$

$$= \frac{\int_{-\infty}^{\infty}\int_{-\infty}^{\infty} C_s(t_1,t_2)\,\frac{\partial}{\partial t_1}\langle S(t_1)\rangle\,\frac{\partial}{\partial t_2}\langle S(t_2)\rangle dt_1 dt_2}{\left[\int_{-\infty}^{\infty}\langle S(t)\rangle\,\frac{\partial^2}{\partial t^2}\langle S(t)\rangle dt\right]^2} \ . \tag{21}$$

As mentioned in the case of two-color ranging [2], Eq.(21) gives the lower bound of the variance in the correlation estimator. The actual timing variance is expected to be higher depending on the actual SNR and owing to nonideality of the delay. Besides, lack of exact information on the aspect of LAGEOS makes us to suppose only a smoothed expected pulse pattern $\bar{S}(t)$, which makes the actual timing variance in the case of single-color ranging greater than that estimated by Eq.(21). Then if we assume $\langle N\rangle$ is so large that we can neglect the first term of $C_s(t_1,t_2)$ in Eq.(8), $\langle\Delta\tau_{COR}{}^2\rangle$ is found to be approximately

$$\frac{\sum_{m}^{M}\sum_{n}^{M}\sum_{m'}^{M}\sum_{n'}^{M}{}_{m\neq n}\sigma_m\sigma_n\sigma_{m'}\sigma_{n'}\left(\frac{\Psi_m+\Psi_n}{2}-\Psi_{m'}\right)\left(\frac{\Psi_m+\Psi_n}{2}-\Psi_{n'}\right)\exp\left[-\frac{(\Psi_m-\Psi_n)^2}{4\sigma_f^2}-\frac{\left(\frac{\Psi_m+\Psi_n}{2}-\Psi_{m'}\right)^2}{4\sigma_g^2}\right]}{4\left\{\sum_{m=1}^{M}\sum_{m'=1}^{M}\left[\frac{(\Psi_m-\Psi_{m'})^2}{4\sigma_g^2}-\frac{1}{2}\right]\sigma_m\sigma_{m'}\exp\left[-\frac{(\Psi_m-\Psi_{m'})^2}{4\sigma_g^2}\right]\right\}^2}. \tag{22}$$

On the other hand, if <N> is not so large, we should retain the first term of Eq.(8) into the integral in Eq.(21). Under the assumption that $\sigma_f >> \sigma_h$, one can reduce the integral due to the first term into the following summation.

$$\frac{2\left(\sum_{n}^{M}\sigma_n\right)\sum_{m}^{M}\sum_{m'}^{M}\sum_{n'}^{M}\sigma_m\sigma_{m'}\sigma_{n'}\left[3\sigma_f^2-(\Psi_m+\Psi_{m'}+\Psi_{n'})(\Psi_m+2\Psi_{m'}+2\Psi_{n'})+9\Psi_{m'}\Psi_{n'}\right]}{9\sqrt{3}\,\langle N\rangle\left\{\sum_{m=1}^{M}\sum_{m'=1}^{M}\left[\frac{(\Psi_m-\Psi_{m'})^2}{4\sigma_g^2}-\frac{1}{2}\right]\sigma_m\sigma_{m'}\exp\left[-\frac{(\Psi_m-\Psi_{m'})^2}{4\sigma_g^2}\right]\right\}^2} \tag{23}$$

to (22). Then we should add this to (22) to evaluate $\langle\Delta\tau_{COR}^2\rangle$ when <N> is not so large and $\sigma_f >> \sigma_h$.

III. APPLICATION TO LASER RANGING WITH THE LAGEOS

Once the information on the lidar cross sections and mutual optical path difference of the CCRs is given, one may readily find the root-mean-square of the timing error of ranging by summation only. Study on lidar cross sections of a CCR array has been done by the present authors [7]. When one estimates the lidar cross section of a CCR on the LAGEOS, he has to consider the following factors. First, the front face of a CCR is tilted from the normal illumination. Second, the triple-corner-mirrors are not coated.. Third, the laser light is linearly polarized. Fourth, there are some manufacturing errors including an intentional error in the dihedral angle. However, an exact

theoretical estimation of the lidar cross section formula in which all the above facts are considered properly is not yet available. As we mentioned in Ref.[7], the intentional error in dihedral angle and other manufacturing errors make the computation of the lidar cross section very difficult. Numerical estimation formulas for such computation was found by the present authors in Ref.[7]. Hence empirical evaluation of its variation deserves our notice [8]. However, for evaluation and analysis of various detection methods for ranging with CCR arrays, a reasonable numerical formula for estimating the lidar cross section of a CCR is needed.

For analysis and evaluation of the timing error, we shall use the results in Ref.[7], in which the above-mentioned first three factors for estimating the lidar cross section were considered in the computer program completed for the first two factors. So in the computer program we are using here, it is assumed that the corner-mirror system is not coated, but it is neglected that the six sectors of the effective reflecting aperture of one CCR reflect the six light components that interfere with each other and consequently make an interference pattern at the receiver site decreasing the lidar cross section irregularly. So the following results should be revised when we incorporate the exact estimation formula in Ref.[7] for the lidar cross section when linearly polarized laser light is illuminated into the computer program.

Here we show in Figures 2, 3 and 4 the expected pulse pattern when we do a ranging experiment with LAGEOS. In Fig. 2, the functions $f_s(t)$ and $f_{sp}(t)$ have been plotted with $\sigma_f = \sigma_h = 20$ psec and with an aspect of the LAGEOS whose south pole is directed to the ground station. The pattern depends on the aspect of the LAGEOS. Pulse patterns in Fig. 3 were obtained with varying pulsewidth with this aspect of LAGEOS. In this case, only 20 CCRs out of 426 can retroreflect by total reflection at the triple mirror system, while 87 CCRS

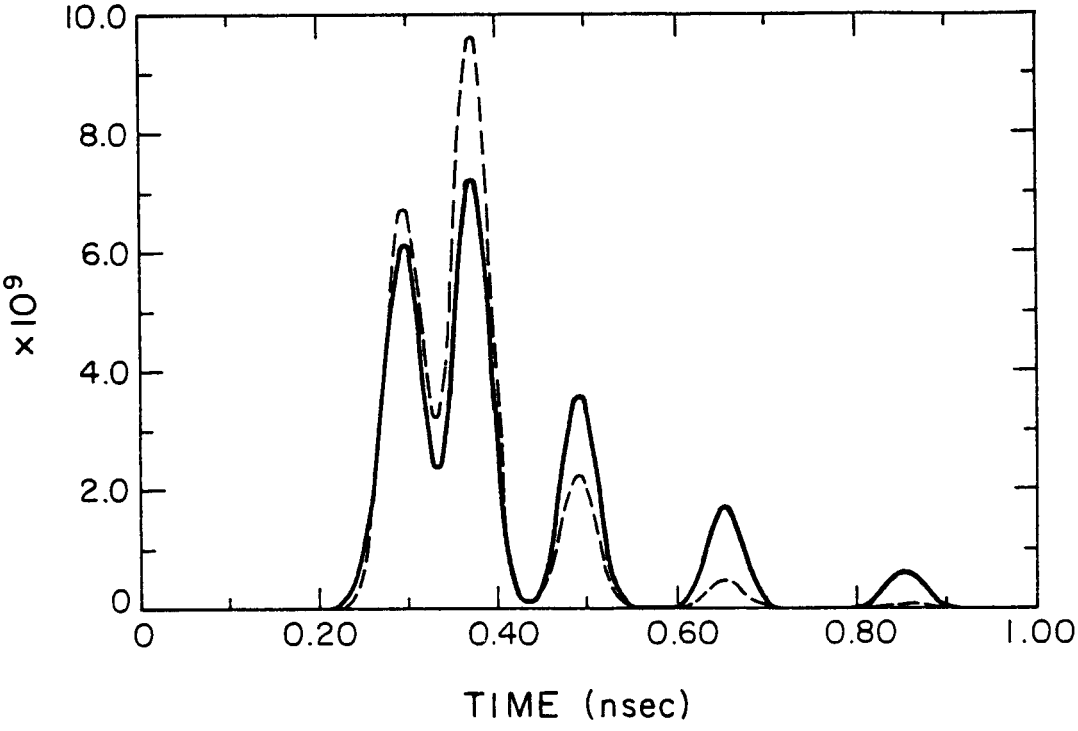

Figure 2. The normalized pulse pattern $f_s(t)$ (solid line) and its speckle function pattern $f_{sp}(t)$ (dashed line) with $\sigma_f = \sigma_h = 20$ nsec when the south pole of LAGEOS directs the ground station.

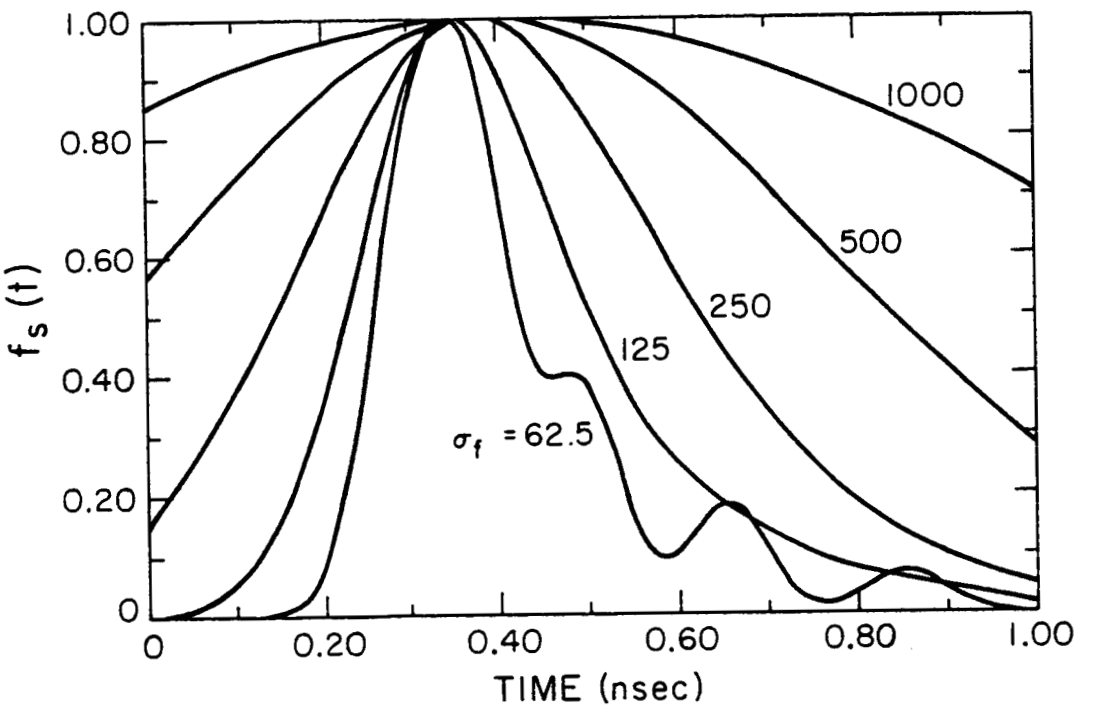

Figure 3. The expected pulse patterns S(t) or $f_s(t)$ that would be obtained after normalizing to each maximum and averaging over the random phase due to speckle and after removing the shot noise of the photodetector. Patterns are drawn with varying pulsewidth σ_f with fixed $\sigma_h = 0$ when the south pole of LAGEOS directs the ground station for the purpose of comparison with those in Ref.[1].

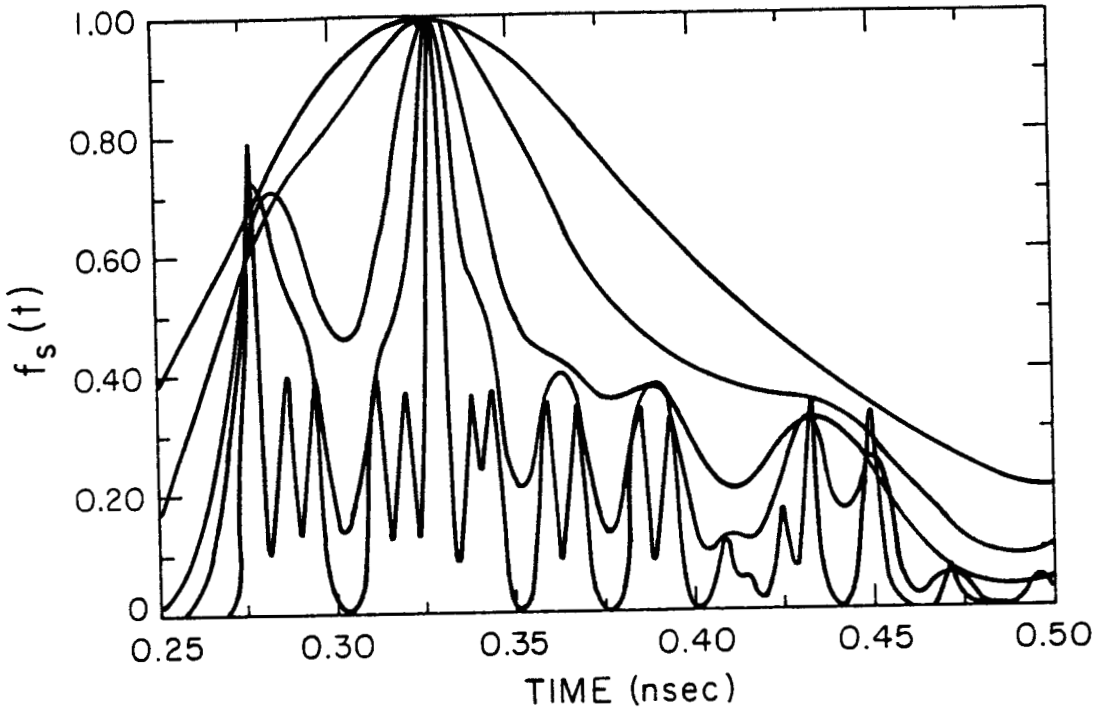

Figure 4. The expected pulse patterns S(t) or $f_s(t)$ that are obtained with varying pulsewidth $\sigma_f = \sigma_h$ when a LAGEOS coordinate (longitude 10^o latitude 85^o) directs to the ground station. According to the order of degree of ruggedness, the patterns are obtained with $\sigma_f = \sigma_h = 2$, 5, 10, 20, 40 psec. The most rugged pattern ($\sigma_f = \sigma_h = 2$ psec) shows the spatially resolved CCRs with a few exceptions at 0.277 and 0.33 psec.

can do so with positive effective retroreflecting areas. Those in Fig. 4 were obtained when the aspect of LAGEOS is quite arbitrary (latitude 85^{o} and longitude 10^{o} on the LAGEOS coordinate) but still fixed with respect to observer. In this case, 23 CCRs can retroreflect the incident light by total reflection, while 99 CCRs can do with positive effective retroreflecting areas. In computing the lidar cross section of each CCR, the velocity aberration effect due to the LAGEOS linear velocity on its orbit has already been considered. That is, the maximum spot of the far-field diffraction pattern was assumed to lie 34 μrad off-axis from the ground station [1]. The former aspect is one of the two aspects of the LAGEOS (that the north of the south pole faces the ground station) with which the light components reflected at different CCRs interferes most severely. On the contrary, the second aspect of the LAGEOS shows a pulse pattern which is virtually uninterferred when the pulsewidth of the laser light and that of the impulse response of the detector is narrow enough to resolve every pule reflected at each CCR. This feature can also be inferred from the timing error analysis.

The SNR and the RMS timing error for each case hae been calculated according to Eqs. (12) and (22) under the assumption that $\langle N \rangle$ is sufficiently large. In Table 1, they are tabulated for the two foregoing aspects of LAGEOS. It was found that, except almost improbable particular aspects, like the first case of the LAGEOS aspect (south or north pole) and like that of Ref.[2] (a flat array of CCRs whose faces direct the laser light exactly), the timing error can be greatly reduced up to the quantum limit when we use extremely short light pulses and an extremely fast photodetector. The RMS values of the timing error in Table 1 were obtained without considering the fundamental limit imposed by wave mechanics. Therefore values less than 10^{-3} psec are theoretical values when the light source with a wavelength much shorter than

TABLE 1. The root-mean-square values of timing error ($\Delta\tau_{COR}$) and the signal-to-noise ratio (R_{SN}) for the two aspects of the LAGEOS with varying σ_f, and σ_h, the pulsewidths of the laser and the photodetector, respectively.
(a) For the aspect that the south pole faces the ground station.

σ_f(psec)	σ_h(psec)	$\Delta\tau_{COR}$(psec)	R_{SN}
0.1	0.1	5.431×10^{-5}	4.4710
1	1	5.431×10^{-5}	4.4710
3	3	8.420×10^{-5}	4.4710
10	10	6.390×10^{-1}	4.3730
20	20	8.08	4.020
62.5	0	32.98	2.0619
125	0	46.07	1.444
250	0	58.98	1.172
500	0	64.29	1.074
1000	0	65.54	1.046

(b) For the aspect that the LAGEOS coordinate - latitude 85^o, longitude 10^o - faces the ground station.

$\sigma_f = \sigma_h$	$\Delta\tau_{COR}$(psec)	R_{SN}
0.1	8.299×10^{-7}	1006.1
1	6.321×10^{-2}	83.263
2	0.1283	59.382
5	2.1235	20.856
10	6.2758	9.4821
20	17.040	4.7458
40	25.161	2.6683

the visible range of wavelength is used. In Appendix A, a computer program is given, which computes the SNR and the RMS timing error and plots the expected pulse pattern $f_s(t)$ and the speckle pattern $f_{sp}(t)$ for a given aspect of LAGEOS and given pulsewidths of the laser and of the photodetector.

CONCLUSIONS

In this report, the correlation estimator for laser ranging with a single-color laser has been studied. Pulse patterns which will be obtained by actual ranging experiment are obtained by simulation with the RMS timing error that will accompany in somewhat idealized experiment. It is idealized because we usually do not know the aspect of the CCR array unless it is fixed. Gaussian approximation has been employed throughout the analysis. That is, the laser pulse and the impulse response of the detector have Gaussian pulse shapes. An expression for the variance of timing error with a given array of CCRs characterized by the lidar cross section and the mutual pathlength differences was found. It was then applied to LAGEOS with somewhat incomplete data on lidar cross sections of each CCR. It is incomplete since the polorization change has not been simulated. It should be revised when the data for correct lidar cross sections is available.

Aside from incomplete datas for the lidar cross section, the timing error analysis has been based on the fact that the expectation of the received signal is fully known. For this statement to be true, we must have complete information of the aspect of LAGEOS, which may hardly be obtained. Therefore the timing error analysis made in this report gives the theoretical limit or lower limit of the timing error. However this work will provide the basis for comparison with other detection techniques and will also provide the way of evaluating various CCR arrays that were and will be developed for ranging application.

The support from NASA for this work is greatly appreciated.

APPENDIX

```
>1,>P
      PROGRAM VEL
C-------------------------------------------------------
C                        G. HUGH SONG updated on FEB. 21, 1987
C     Plots the signal pulse shape function Fs(t)
C     and the speckle pulse shape function Fsp(t).
C    along with the root mean square error of ranging.
C    The velocity aberation is considered in this program.
C    Finally, the rms ranging error (RMSERR) is calculated.
C
C     ASPECT ANGLES : INCIDENCE AND POLARIZATION ANGLES OF LIGHT
C        IN THE LAGEOS COORDINATE SYSTEM
C       ALA (LATTITUDE), ALO (LONGITUDE), DPON IN deg.
C       H (HORRIZONTAL), V (VERTICAL), PON IN radian.
C
C     THE VELOCITY ANGLE
C       DVDN(deg), VDN(rad) : MEASURED W.R.T. THE NORTH POLE
C
C     THE LIDAR SYSTEM PARAMETERS ARE DEFINED IN STATEMENT #302
C     PHI, GAM, & POL ARE DEFINED IN SUBROUTINE SUBCCR
C-------------------------------------------------------
      DIMENSION RANGE(4),FSY(201,1),FSPY(201,1)
      COMMON /PULBLOCK/SIGF(10),SIGH(10),SNR(10),RMSERR(10),
     +    NOCCR,NEFCCR, PTHMI, PTHMA,
     +    R,C,COV,SIV,H,COH,SIH,LPOL,LFRESN,PON,VEL,VDN
      COMMON /GRABLOCK/T(201),FS(10,201),FSP(10,201)
      DATA C/2.9979E8/
      RAD(DEG)=ATAN(1.)*DEG/45.
C-------------------------------------------
      CALL LAGEOS(R)
C-------------------------------------------
  1   WRITE(3,)"INPUT THE PLOTTING TIME RANGE TI & TF IN nsec."
      READ(3,)TI,TF
       TI=TI*1.E-9
       TF=TF*1.E-9
C
      NG=0
  2   NG=NG+1     !GO TO loop count
      IF(NG.EQ.1) GO TO 3
      WRITE(3,)" WILL YOU USE THE SAME TIME SCALE? Y-1, N-0!"
      READ (3,) NY
      IF(NY.EQ.0) GO TO 1
      WRITE(3,256)
 256  FORMAT(" Will you use the same ASPECT OF THE LAGEOS,",/,
     +"          the same VELOCITY DIRECTION,",/,
     +"          and the same POLARIZATION OF THE LASER? Yes-1, No-0")
      READ(3,)NY
      IF(NY.EQ.1) GO TO 204
C
  3   WRITE(3,301)
 301  FORMAT(/" INPUT THE ASPECT ANGLE OF THE LAGEOS!",//,
     +" THE LONGITUDE (DEGREES) (0. =< ALA =< 360.)")
      READ(3,)ALA
      WRITE(3,)" THE LATTITUDE (DEGREES) (-90. =< ALO < 90.)"
      READ(3,)ALO
      H=RAD(ALA)
      V=RAD(ALO)
      COV=COS(V)
      SIV=SIN(V)
      COH=COS(H)
      SIH=SIN(H)
C
      WRITE(3,)
     +" INPUT THE VELOCITY DIRECTION W.R.T. THE NORTH POLE IN deg!"
      READ(3,)DVDN
      VDN=RAD(DVDN)
C----------------------
      WRITE(3,375)
 375  FORMAT(" ARE YOU GOING TO CONSIDER THE FRESNEL REFLECTION",/,
     +" INSIDE THE CCR AS WELL AS THE TOTAL REFLECTION?",/
     +" It will take 20 min/set of plots. Yes-1, No-0.",/)
      READ(3,) LFRESN
C
      WRITE(3,306)
```

```
  306  FORMAT(/,/," IS THE INCIDENT LIGHT POLARIZED?  YES-1, NO-0")
  202  READ(3,) LPOL
       IF(LPOL)203,204,203
C
  203  WRITE(3,308)
  308  FORMAT(/" Sorry. Not developed for polarized light."/,
      +" The program assumes unpolarized light in the following.")
C     +" WE SHALL ASSUME THAT THE LIGHT IS LINEARLY POLARIZED.",/,
C     +" SPECIFY THE DIRECTION OF THE POLARIZATION IN deg.",/,
C     +" SO THAT DPON=0. MEANS E-FIELD ALONG THE NORTH-SOUTH"
C     +,/," DIRECTION OF THE LAGEOS.")
C      READ(3,)DPON
C      PON=RAD(DPON)
C
  204  WRITE(3,302)
  302  FORMAT(//," INPUT THE LIDAR SYSTEM PARAMETERS!",//
      +" SIGF(sec) : RMS LASER PULSE WIDTH,",/
      +" SIGH(sec) : RMS WIDTH OF THE RECEIVER IMPULSE RESPONSE.",///
      +" How many diff. set of SIGF & SIGH do you want? JC = ?")
       READ (3,) JC
       WRITE(3,309) 2.E9*R/C
  309  FORMAT(//" Note that  2*Radius/C = ",G13.6," nsec.",/,
     +" Input SIGF and SIGH in psec line by line for each set!")
C
       DO 229 J=1,JC
       READ(3,) SIGF(J), SIGH(J)
        SIGF(J)=SIGF(J)*1.E-12
  229   SIGH(J)=SIGH(J)*1.E-12
C
       DO 55 IT=1,201
   55  T(IT)=TI+(IT-1)/200.*(TF-TI)
C
C--------------------DO LOOP FOR SETS OF Fs(t) and Fsp(t)----
C
       DO 9999 J=1,JC
C
       CALL PULSEPAT(J)
C
 9999  CONTINUE
C
C-----------------------------END  of the DO LOOP----
C
       WRITE(77,)JC,NOCCR,NEFCCR,PTHMI,PTHMA
       DO 175 J=1,JC
  175  WRITE(77,)SIGF(J),SIGH(J),SNR(J),RMSERR(J)
       RANGE(1)=T(1)
       RANGE(2)=T(201)
       RANGE(3)=0.
       RANGE(4)=0.
C
  377  WRITE(3,)" J = what d'yu plot on screen? If J=0, no plot."
       READ(3,) J
       WRITE(3,352)1.E12*SIGF(J),1.E12*SIGH(J)
  352  FORMAT(1X,"LASER PULSEWIDTH : SIGF=",G16.7,"psec.",/,
      +" RECEIVER IMP.RESP. PULSEWIDTH :SIGH=",G16.7,"psec.",//)
       IF(J.EQ.0) GO TO 120
C
       DO 119 I=1,201
       FSY(I,1)=FS(J,I)
  119  FSPY(I,1)=FSP(J,I)
C
       CALL USPLO(T,FSY,201,201,1,1,5HFs(t),
      +           4,4HTIME,4,5HFs(t),5,RANGE,1H1,0,IER)
       CALL USPLO(T,FSPY,201,201,1,1,6HFsp(t),6,
      +     4HTIME,4,6HFsp(t),6,RANGE,1H1,0,IER)
C
  120  WRITE(3,51)RMSERR(J)*1.E12,SNR(J),NEFCCR,NOCCR,1.E9*PTHMI,1.E9
     + *PTHMA
   51  FORMAT(///" THE RMS ERROR OF RANGING IS ",G10.3,"psec.",//,
      +" THE SIGNAL-TO-NOISE RATIO IS ",G10.3,//,
      +" The total No. of effectively reflecting CCRs is ",I3,//,
      +" The total No. of CCRs with positive ref. area is ",I3,/,
      +" <--  not valid when you dont consider Fresnel ref.",//
      +"  from PTHMI=",G10.3,"nsec to PTHMA=",G10.3,"nsec.",///)
```

```
C-------------------------------------
      WRITE(3,)" Another plot in the screen? Yes-1, No-0."
      READ (3,) NY
      IF(NY.EQ.1) GO TO 377
 379  WRITE(3,)" Destroy current data and get new? Yes-1, No-0."
      READ(3,)NY
      IF(NY.GE.1) GO TO 2
C
      WRITE(3,)" WANT TO PLOT ON THE ELECTOSTATIC PLOTTER? Y-1,N-0"
      READ(3,) NY
      IF(NY.EQ.0) GO TO 999
C
      WRITE(3,31)
 31   FORMAT(" WHAT DO YOU WANT TO PLOT?",/
     +" 1 set of Fs(t) and Fsp(t)?  Then type No. of the set J!",/,
     +" Several(.LE.ten) Fs(t)'s on the same scale? Type 11!",/,
     +" OR do you want to stop?   Type 999!")
      READ (3,) J
      IF(J.LE.10) CALL GRAPHICS(J)
      IF(J.EQ.11) CALL MULTIGRA(JC)
      IF(J.EQ.999) STOP
      GO TO 379
 999  STOP
      END
C
CC=================================================
C
      SUBROUTINE PULSEPAT(J)
C
CCCCCC
C     XSC(m)  : CROSS SECTION OF THE m-TH CCR
C     SXSC    : TOTAL SUM OF XSC(m)'S
C     SPGAM   : INTERFERENCE FACTOR FOR EACH CCR
C     SGAM    : WEIGHTED SUM OF SPGAM'S
CCCCCC
C-------------------------------------------------
      DIMENSION XSC(426),PTH(426)
      COMMON /GRABLOCK/T(201),FS(10,201),FSP(10,201)
      COMMON /PULBLOCK/ SIGF(10),SIGH(10),SNR(10),RMSERR(10),
     +  NOCCR, NEFCCR,PTHMI,PTHMA,
     +  R,C,COV,SIV,H,COH,SIH,LPOL,LFRESN,PON,VEL,VDN
      COMMON /LAGE/X(426),Y(426),Z(426),THE(426),PSI(426),ORI(426)
      COMMON /BOARDER/PHI,TAP
      DATA XSC,PTH/852*0./
      DATA DIST,VP/5.9E+6, 34.E-6/
      DATA RI,VT,DIA,WL/1.455, .0278, .0381, 5.32E-7/
      DATA NOCCR,NEFCCR/2*07
C
      RAD(DEG)=ATAN(1.)*DEG/45.
      PI=4.*ATAN(1.)
C
      SQSG4=4.*(SIGF(J)**2+SIGH(J)**2)
      SIGG=SQRT(SQSG4)/2.
C-----------------------Compute Fs(t).
      PTHMI=R/C
      PTHMA=0.
      SXSC=0.
      SGAM=0.
C
      DO 81 N=1,426
      RTHE=RAD(THE(N))
      RPSI=RAD(PSI(N))
      RORI=RAD(ORI(N))
      COPHI=(COV*(COH*X(N)+SIH*Y(N))+SIV*Z(N))/R
      IF(COPHI.LE.0.) GO TO 80
      IF(COPHI.GE.1.)PHI=0.
      IF(COPHI.LT.1.)PHI=ACOS(COPHI)
      GAM=ATAN(COV*SIN(RPSI-H)/(SIV*SIN(RTHE)-COV
     +      *COS(RTHE)*COS(RPSI-H)))-RORI
      ZET=ATAN(SIN(RTHE)*SIN(H-RPSI)/(COS(RTHE)*COV-SIN(RTHE)
     +      *SIV*COS(H-RPSI)))
      IF(LPOL.EQ.1)
      POL=PON-PI/2.+ZET   ! TE ANGLE FOR EACH CCR (POL=0 : TE)
      ELSE
       POL=PI/4.
```

```
222:          END IF
223:          VEL=VDN-ZET
224:    C      !VEL : VELOCITY ANGLE FOR EACH CCR(VEL=0 : SHORT AXIS=x-AXIS)
225:          RK=4.*VP*PI/WL/DIST/DIA          !VP : MAX ABERATION ANGLE(rad)
226:          XK=RK*COS(VEL)
227:          YK=RK*SIN(VEL)
228:    C
229:          CALL SUBCCR(1.455,GAM,PHI,0,0,LFRESN,POL,ALP,BET,
230:         +     DPHIM,ARN,TOTREF,REF,TOP)
231:    C
232:          IF(REF.EQ.0.) GO TO 80
233:          NOCCR=NOCCR+1
234:          IF(TOTREF.GT.0.) NEFCCR=NEFCCR+1
235:    C           \Count the No. of effective CCRs.
236:          CALL FT2D(XK,YK,.01,TOP,FT)
237:    C
238:          XSC(N)=FT*FT*REF  ! Velocity aberation effect
239:          PTH(N)=2.*(R*(1.-COPHI)+VT*SQRT(RI*RI-1.+COPHI*COPHI))/C
240:    C           !REFLECTION TIME CORRECTION FOR EACH CCR
241:           PTHMI=AMIN1(PTHMI,PTH(N))
242:           PTHMA=AMAX1(PTHMA,PTH(N))
243:    C           \The first and last CCRs' locations in time.
244:          DO 98 IT=1,201
245:          TIPN=T(IT)-PTH(N)
246:     98   FS(J,IT)=FS(J,IT)+XSC(N)*EXP(-TIPN*TIPN/SIGG**2)/SIGG/SQRT(PI)
247:          GO TO 81
248:     80   XSC(N)=0.
249:     81   SXSC=SXSC+XSC(N)
250:    C
251:    C-------------------------Compute Fsp(t) the the timing error.
252:          RMSDEN=-XSC(1)*XSC(1)/2.
253:          RMSNOM=0.
254:          NACC=1
255:    C
256:          DO 85 N=2,426
257:          IF(XSC(N).EQ.0.)GO TO 85
258:          NACC=NACC+1
259:          WRITE(3,)J,NACC,N
260:          RMSDEN=RMSDEN-XSC(N)*XSC(N)/2.
261:          NM1=N-1
262:    C
263:          DO 84 M=1,NM1
264:          IF(XSC(M).EQ.0.)GO TO 84
265:          TD=PTH(M)-PTH(N)
266:          TM=(PTH(M)+PTH(N))/2.
267:          SPGAM=XSC(M)*XSC(N)*EXP(-TD*TD/4./SIGF(J)/SIGF(J))
268:          SGAM=SGAM+2.*SPGAM
269:          RMSDEN=RMSDEN+2.*XSC(M)*XSC(N)*(TD*TD/SQSG4-.5)
270:         +       *EXP(-TD*TD/SQSG4)
271:    C
272:          DO 87 IT=1,201
273:          TITM=T(IT)-TM
274:     87   FSP(J,IT)=FSP(J,IT)+2.*SPGAM
275:         +       *EXP(-TITM*TITM/SIGG/SIGG)/SIGG/SQRT(PI)
276:    C
277:          DO 88 NP=1,426
278:          IF(XSC(NP).EQ.0.)GO TO 88
279:          TPN=TM-PTH(NP)
280:          CSNOM=0.
281:    C
282:          DO 89 MP=1,NP
283:          IF(XSC(MP).EQ.0.)GO TO 89
284:          TPM=TM-PTH(MP)
285:          SNOM=XSC(MP)*TPM*EXP(-TPM*TPM/SQSG4)
286:          IF(NP.EQ.MP)SNOM=SNOM/2.
287:          CSNOM=CSNOM+SNOM
288:     89   CONTINUE
289:          RMSNOM=RMSNOM+CSNOM*2.*XSC(NP)*TPN*SPGAM
290:         +       *EXP(-TPN*TPN/SQSG4)
291:     88   CONTINUE
292:     84   CONTINUE
293:     85   CONTINUE
294:    C
295:          SNR(J)=SXSC*SXSC/SGAM
```

```
      RMSNOM=RMSNOM/SGAM/4.
      RMSDEN=RMSDEN/SXSC
      RMSERR(J)=ABS(SQRT(RMSNOM/SNR(J))/RMSDEN)
C-----------------Normalize Fs(t) and Fsp(t).
      DO 97 IT=1,201
       FS(J,IT)=FS(J,IT)/SXSC
 97    FSP(J,IT)=FSP(J,IT)/SGAM
      DO 83 I=1,201
C     WRITE(66,310)T(I),FS(J,I)
 83   WRITE(66,)T(I),FS(J,I),FSP(J,I)
C310  FORMAT(2(1X,G16.7))
C
      RETURN
      END
C
CC=====================================================================
C
      SUBROUTINE LAGEOS(R)
C
CCC   PRODUCES SIX ARRAYS OF COORDINATES AND ORIENTATIONS
CCC   AND THE COMMON RADIUS OF ALL 426 CCR'S.
CCC
CCC   X,Y,Z: CARTESIAN COORDINATES
CCC   SPHERICAL COORDINATES
CCC     R   : THE COMMON RADIUS
CCC     THE: LONGITUDE (NORTH POLE : THE=0.)
CCC     PSI: LATITUDE
CCC   ORI   : ORIENTATION OF ONE EDGE OF A CCR
C-----------------------------------------------
      DIMENSION DTHE(20),DORI(20),BETW(20), NUM(20)
      COMMON /LAGE/X(426),Y(426),Z(426),THE(426),PSI(426),ORI(426)
      DATA NUM/1,2,8,20,38, 61,88,119,150,182,
     +         214,246,278,309,340, 367,390,408,420,426/
      DATA DTHE/0., 10.118, 19.848, 29.579,  39.309,
     +    49.039,  58.769, 67.018,  76.748,   85.135,
     +   94.865,  103.252, 112.982, 121.231, 130.961,
     +  140.691,  150.421, 160.151, 169.881, 180./
      DATA DORI/55., 91., 43., 31., 29., 11., 97., 63., 55., 47.,
     +          94.,102.,110., 24., 58., 76., 78., 90., 18., 102./
      DATA BETW/7*0., 1., 0., 1., 1., 0., 1., 7*0./
      PI=4.*ATAN(1.)
      R=.2721
C
      DO 887 J=1,426
      DO 888 I=1,19
      NU=NUM(I+1)
      IF(J.LT.NU)GO TO 889
 888  CONTINUE
C
 889  THE(J)=DTHE(I)
      PSI(J)=(J-NUM(I)+.5*BETW(I))*360./(NUM(I+1)-NUM(I))
      ORI(J)=DORI(I)-26.*(J-NUM(I))
 10   IF(ORI(J).GE.0.)GO TO 20
      ORI(J)=ORI(J)+120.
      GO TO 10
 20   RPSI=PSI(J)*PI/180.
      RTHE=THE(J)*PI/180.
      X(J)=R*SIN(RTHE)*COS(RPSI)
      Y(J)=R*SIN(RTHE)*SIN(RPSI)
887   Z(J)=R*COS(RTHE)
      RETURN
      END
C
CC=====================================================================
C
      SUBROUTINE FT2D(X,Y,B,TOP,FT)
C.....................................
CCC              G. HUGH SONG, updated on APRIL 15, 1986
CCC   SLO : SLOPE OF EACH LINEARIZED TRAPEZOID
CCC   TOP : THE TOP POINT OF THE PUPIL
CCC   B   : THE HEIGHT OF THE TRAPEZOID
CCC   BP  : THE HEIGHT OF THE ISOSCELES
CCC   X,Y : THE SPATIAL FREQUENCY
C-----------------------------------------------
```

```
370:          N=IFIX(TOP/B)
371:          BP=TOP-N*B
372:          SLO=-F(N*B)/BP
373:          TMB=TOP-BP
374:          TMB2=TOP-BP/2.
375:          IF(X.EQ.0.)
376:           FT=2.*SLO*BP*(TMB*SINK(2.*Y*TMB)
377:         +                -TMB2*SINK(2.*Y*TMB2)*SINK(BP*Y))
378:           ELSE
379:           YPX=Y+X*SLO
380:           YMX=Y-X*SLO
381:           FT=2./X*BP*(SIN(TMB2*Y-SLO*BP*X/2.)*SINK(BP*YPX)
382:         +   -SIN(TMB2*Y+SLO*BP*X/2.)*SINK(BP*YMX))
383:           END IF
384:    C
385:          DO 99 I=1,N
386:          BM=(I-.5)*B
387:          SLO=(F(I*B)-F((I-1)*B))/B
388:          FM=(F(I*B)+F((I-1)*B)+2.*F(BM))/4.
389:          IF(X.EQ.0.)
390:           FT=FT+4.*B*(FM*SINK(B*Y)*COS(Y*BM)
391:         +             +SLO*BM*SINK(2.*Y*BM)*(COS(B*Y/2.)-SINK(B*Y)))
392:           ELSE
393:          YMX=Y-X*SLO
394:          YPX=Y+X*SLO
395:           FT=FT+2./X*B*(SIN(X*FM+Y*BM)*SINK(B*YPX)
396:         +              +SIN(X*FM-Y*BM)*SINK(B*YMX))
397:           END IF
398:     99   CONTINUE
399:    C
400:          RETURN
401:          END
402:    C
403:          FUNCTION SINK(Z)
404:          IF(Z.EQ.0.)
405:            SINK=1.
406:            ELSE
407:            SINK=SIN(Z/2.)*2./Z
408:           END IF
409:          RETURN
410:          END
411:    C=============================================================
412:          FUNCTION F(Y)
413:          COMMON /BOARDER/PHI,TAP
414:          F=COS(PHI)*(SQRT(1.-Y*Y)-SQRT(2.)*TAP)
415:          RETURN
416:          END
417:    C
418:    C=============================================================
419:    C
420:          SUBROUTINE GRAPHICS(J)
421:    C
422:          DIMENSION X1(201),Y1(201),Y2(201)
423:          COMMON /GRABLOCK/ T(201),FS(10,201),FSP(10,201)
424:          DATA Y2M/0./
425:    C
426:          DO 1 I=1,201
427:          X1(I)=T(I)*1.E+9
428:          Y2(I)=FSP(J,I)/1.E+9
429:          Y2M=AMAX1(Y2M,Y2(I))
430:      1   Y1(I)=FS(J,I)/1.E+9
431:          WRITE(3,301) Y2M
432:     301  FORMAT(" Max of graph=",G10.3," Set it again for a nice plot."
433:         +,/," Make it a little larger than the original max. Ymax=?")
434:          READ(3,) Y2M
435:    C
436:          CALL PINIT(1.5, 5., 201)
437:          CALL MGRPHL(X1,Y2,201, X1(1), X1(201),0., Y2M, 6.,4.)
438:          CALL DATPL2(X1,Y1,201,0,1,0,0.,0,4,0)
439:          CALL TITLE(1HL,5H1.E+9,5,.14,1)
440:          CALL TITLE(1HB,11HTIME (nsec),11,.14,1)
441:          CALL WHERE
442:          RETURN
443:          END
```

```
C=============================================================
      SUBROUTINE MULTIGRA(NG)
      COMMON /GRABLOCK/X(201),Y(10,201),Z(10,201)
      DIMENSION YG(201), YM(5)
      DATA YM/5*0./
C-----------------------------------SCALING----
      DO 3 J=1,NG
      DO 3 I=1,201
    3 YM(J)=AMAX1(YM(J),Y(J,I))
C
      DO 5 I=1,201
      DO 4 J=1,NG
    4 Y(J,I)=Y(J,I)/YM(J)
    5 X(I)=X(I)*1.E9
C-------------------------------PLOT----
      CALL PINIT(1.5, 5., 1000)
      DO 7 I=1,201
    7 YG(I)=Y(1,I)
      CALL MGRPHL(X,YG,201,X(1),X(201), 0., 1., 6., 4.)
      IF(NG.EQ.1) GO TO 999
C
      DO 6 J=2,NG
      DO 8 I=1,201
    8 YG(I)=Y(J,I)
    6 CALL DATPL2(X,YG,201,0,1,0,0.,0,2,0)
      CALL TITLE(1HL,5HFs(t),5,.14,1)
      CALL TITLE(1HB,11HTIME (nsec),11,.14,1)
      CALL WHERE
  999 RETURN
      END
C
      SUBROUTINE SUBCCR(RI,GAM,PHI,LFACE,LCOAT,LFRESN,POL,
     + ALP,BET,   DPHIM,ARN,REF,REFFR,TOP)
CCCCCCCCCCCCCCCCCCCCCCCCCCCCCCCCCCCCCCCCCCCCCCCCCCCCCCCCCCCCCCCCC
C                                 G. HUGH SONG, FEB. 21, 1987
C
C     COMPUTES THE REFLECTANCE OF A CUBE CORNER RETROREFLECTOR
C     FROM SPECIFIED DATA OF THE RI, GAM, PHI ANGLES.
C
C     RI: Refractive index of the CCR.
C     GAM(rad):Angle of the plane of incidence
C        It is measured from one edge direction (north pole).
C     PHI: angle of incidence to the front face of the CCR.
C     LFACE: If 1, it has a hexagonal face, or if 0, a circular face
C     LCOAT: If 1, the CCR is coated, if 0, uncoated.
C     POL:  angle of polarization axis, POL=0. and POL=PI/2. mean
C           the TM and TE incidence, respectively.
C     BET=ANGLE OF PASSIVE ROTATION WITH RESPECT TO THE Z AXIS
C     ALP=ANGLE OF PASSIVE ROTATION WITH RESPECT TO THE Y-PRIME AXIS
C     DPHIM=MAX ACCEPTANCE ANGLE OF INCIDENCE TO REACH THE VERTEX
C     ARN=NORMALIZED EFFECTIVE REFLECTING AREA
C     REF=REFLECTANCE FOR INTENSITY
C
C     Be sure to use the P option in SAUF77 compilation.
C-------------------------------------------------------------
      COMMON /ALBE/SIA,COP,RT2,SIP,RT3,COA,TAA,PI
C
      REF=0.
      REFFR=0.
      ARN=0.
      RT2=SQRT(2.)
      RT3=SQRT(3.)
      PI=4.*ATAN(1.)
      SIP=SIN(PHI)/RI
      PH=ASIN(SIP)
C           !PH=angle of transmitted light through the front face
      COP=COS(PH)
      TAP=SIP/COP
      COCP=COS(PHI)
C---------------Check the visibility of the vertex.
      IF(LFACE.EQ.0)
       TAPM=1./RT2
       ELSE
       TAPM=1./RT2/COS(AMIN1(ABS(PI/3.-GAM),ABS(PI-GAM),ABS(5.*PI/3.
```

ORIGINAL PAGE IS
OF POOR QUALITY

```
     +    -GAM)))
      END IF
C
      SIPM=SIN(ATAN(TAPM))*RI
      DPHIM=90.
      IF(SIPM.LT.1.)DPHIM=ASIN(SIPM)*180./PI
      IF(TAP.GE.TAPM)RETURN  !REF=0. is to be returned.
C
      CALL ALPBET(GAM,ALP,BET)
C
C-------------------------------------------------
C           COMPUTATION OF AREA
C.................................................
      GAMS=AMIN1(ABS(GAM), ABS(GAM-2.*PI/3.), ABS(GAM-4.*PI/3.),
     +           ABS(2.*PI-GAM))
      CALL ALPBET(GAMS,ALPS,BETS)
C
      SIB=SIN(BETS)
      COB=COS(BETS)
C
      IF(LFACE.EQ.0)
       ARN=2./PI*COCP*(ACOS(RT2*TAP)-RT2*TAP*SQRT(1.-2.*TAP*TAP))
       TOP=SQRT(1.-2.*TAP*TAP)
      ELSE IF(LFACE.EQ.1)
       AREA=4.*SIB*COB*COA/TAA
       IF(TAA.LE.(2.*COB)) AREA=SIB*(4.*COA-SIA/COB)
       IF(TAA.LE.COB) AREA=SIB*COA*(4.-COB/TAA)
       IF(TAA.LE.SIB)WRITE(3,)"ERR??"
C       AREA=SIA*(4.-COB/SIB)
C       IF((2.*SIB).LT.COB) AREA=4.*SIA*SIB/COB
       AREA=AREA*COCP/COP
       ARN=AREA/RT3
      END IF
C
      IF(ARN.LE.0.)
       WRITE(3,) " Negative ARN???  Error!! ARN = ",ARN
       ARN=0.
       RETURN
      END IF
      IF(LCOAT.EQ.1) GO TO 39
C-------------------------------------------------------
C         CHECK THE TOTAL REFLECTION
C
      COSTH=SQRT(1.-1./RI/RI)
      COMIN=AMAX1(COB*COA,SIB*COA,SIA)
      IF((COMIN.GE.COSTH).AND.(LFRESN.EQ.0)) RETURN
C-------------------------------------------------
C       CALCULATION OF  REFLECTANCE (REF)
C       NORMALIZED TO THE CASE OF NORMAL INCIDENCE
C.................................................
 39   TITE=2.*COCP/(COCP+RI*COP)
      TITM=2.*COCP/(RI*COCP+COP)
      TOTE=2.*RI*COP/(RI*COP+COCP)
      TOTM=2.*RI*COP/(COP+RI*COCP)
       TMC=SIN(POL) !TM-component
       TEC=COS(POL) !TE-COMPONENT
       REF=((TEC*TITE)**2+(TMC*TITM)**2)
C  TEC & TMC should be redefined for exit wave in the future
       REF=REF*((TEC*TOTE)**2+(TMC*TOTM)**2)
      REFFR=REF
      IF(LCOAT.EQ.1) GO TO 31
C-------------------------------------------------------------
C         and consider Fresnel reflection in triple corner mirror.
C
C
      IF(COMIN.GE.COSTH) THEN
      THI=ACOS(COMIN)
C               \ Incident ang. to transm. corner mirror
      THT=ASIN(SIN(THI)*RI)
C                \ Transm. ang. out of the corner mirror
      RTE=TAN(THI-THT)/TAN(THI+THT)
      RTM=-SIN(THI-THT)/SIN(THI+THT)
C    \ For polarized input, TEC and TMC should be redefined in future
      REFFR=REF*((RTE*TEC)**2+(RTM*TMC)**2)
```

```
592:          REF=0.
593:          END IF
594:    31    CONTINUE
595:    C-----------------NO NORMALIZATION w.r.t. NORMAL INCIDENCE.
596:    C     REF=REF/(4.*RI/(RI+1.)/(RI+1.))**2
597:    333   RETURN
598:          END
599:    C
600:    C=======================================
601:    C
602:          SUBROUTINE ALPBET(GAM,ALP,BET)
603:          COMMON /ALBE/SIA,COP,RT2,SIP,RT3,COA,TAA,PI
604:    C-------------------------------
605:    C        COMPUTE ALP & BET !
606:    C-------------------------------------------------------------------
607:          COG=COS(GAM)
608:          SIA=(COP+RT2*SIP*COG)/RT3
609:          ALP=ASIN(SIA)
610:          COA=COS(ALP)
611:          TAA=SIA/COA
612:          SBOR2=(RT3*COP-SIA)/COA/RT2      !SIN(BET)+COS(BET)=RT2*SBOR2
613:          IF(SBOR2.GE.1.)GO TO 600
614:          BET=PI/4.+ACOS(SBOR2)
615:          IF(GAM.LT.PI) BET=PI/2.-BET
616:          GO TO 700
617:    600   BET=PI/4.
618:    700   RETURN
619:          END
620:    C
621:    C=====================================================
622:    C
```

```
>1,>P
      PROGRAM POSTVEL
C-------------------------------------------------------
C                    G. HUGH SONG updated on FEB. 21, 1987
C     Plots the signal pulse shape function Fs(t)
C     and the speckle pulse shape function Fsp(t).
C    along with the root mean square error of ranging.
C    The velocity aberation is considered in this program.
C    Finally, the rms ranging error (RMSERR) is calculated.
C
C     THIS PROGRAM RESUMES TGHE WORK VEL AFTER A WHILE
C
C-------------------------------------------------------
      DIMENSION RANGE(4),FSY(201,1),FSPY(201,1)
      DIMENSION SIGF(10),SIGH(10),SNR(10),RMSERR(10)
      COMMON /GRABLOCK/T(201),FS(10,201),FSP(10,201)
      DATA C/2.9979E8/
      RAD(DEG)=ATAN(1.)*DEG/45.
C-------------------------------------------
      READ(77,)JC,NOCCR,NEFCCR,PTHMI,PTHMA
      DO 175 J=1,JC
      DO 174 I=1,201
 174  READ(66,)T(I),FS(J,I),FSP(J,I)
 175  READ(77,)SIGF(J),SIGH(J),SNR(J),RMSERR(J)
C
      RANGE(1)=T(1)
      RANGE(2)=T(201)
      RANGE(3)=0.
      RANGE(4)=0.
C
 377  WRITE(3,)" J = what d'yu plot on screen? If J=0, no plot."
      READ(3,) J
      WRITE(3,352)1.E12*SIGF(J),1.E12*SIGH(J)
 352  FORMAT(1X,"LASER PULSEWIDTH : SIGF=",G16.7,"psec.",/,
     +" RECEIVER IMP.RESP. PULSEWIDTH :SIGH=",G16.7,"psec.",//)
      IF(J.EQ.0) GO TO 120
C
      DO 119 I=1,201
      FSY(I,1)=FS(J,I)
 119  FSPY(I,1)=FSP(J,I)
C
      CALL USPLO(T,FSY,201,201,1,1,5HFs(t),
     +           4,4HTIME,4,5HFs(t),5,RANGE,1H1,0,IER)
      CALL USPLO(T,FSPY,201,201,1,1,6HFsp(t),6,
     +     4HTIME,4,6HFsp(t),6,RANGE,1H1,0,IER)
C
 120  WRITE(3,51)RMSERR(J)*1.E12,SNR(J),NEFCCR,NOCCR,1.E9*PTHMI,1.E9
     +    *PTHMA
 51   FORMAT(///" THE RMS ERROR OF RANGING IS ",G10.3,"psec.",//,
     +" THE SIGNAL-TO-NOISE RATIO IS ",G10.3,//,
     +" The total No. of effectively reflecting CCRs is ",I3,//,
     +" The total No. of CCRs with positive ref. area is ",I3,//,
     +"  from PTHMI=",G10.3,"nsec to PTHMA=",G10.3,"nsec.",///)
C-------------------------------------
 379  WRITE(3,)" Another plot in the screen? Yes-1, No-0."
      READ (3,) NY
      IF(NY.EQ.1) GO TO 377
C
      WRITE(3,)" WANT TO PLOT ON THE ELECTOSTATIC PLOTTER? Y-1,N-0"
      READ(3,) NY
      IF(NY.EQ.0) GO TO 999
C
      WRITE(3,31)
 31   FORMAT(" WHAT DO YOU WANT TO PLOT?",/
     +" 1 set of Fs(t) and Fsp(t)?  Then type No. of the set J!",/,
     +" Several(.LE.ten) Fs(t)'s on the same scale? Type 11!",/,
     +" OR do you want to stop?   Type 999!")
      READ (3,) J
      IF(J.LE.10) CALL GRAPHICS(J)
      IF(J.EQ.11)
       WRITE(3,)" How many (JC) curves, J=1,...,JC, JC=?"
       READ(3,) JC
       CALL MULTIGRA(JC)
      END IF
```

```
      IF(J.EQ.999) STOP
      GO TO 379
  999 STOP
      END
C
C=============================================================
C
      SUBROUTINE GRAPHICS(J)
C
      DIMENSION X1(201),Y1(201),Y2(201)
      COMMON /GRABLOCK/ T(201),FS(10,201),FSP(10,201)
      DATA Y2M/0./
C
      DO 1 I=1,201
      X1(I)=T(I)*1.E+9
      Y2(I)=FSP(J,I)/1.E+9
      Y2M=AMAX1(Y2M,Y2(I))
    1 Y1(I)=FS(J,I)/1.E+9
      WRITE(3,301) Y2M
  301 FORMAT(" Max of graph=",G10.3," Set it again for a nice plot."
     +,/," Make it a little larger than the original max. Ymax=?")
      READ(3,) Y2M
C
      CALL PINIT(1.5, 5., 201)
      CALL MGRPHL(X1,Y2,201, X1(1), X1(201),0., Y2M, 6.,4.)
      CALL DATPL2(X1,Y1,201,0,1,0,0.,0,4,0)
      CALL TITLE(1HL,5H1.E+9,5,.14,1)
      CALL TITLE(1HB,11HTIME (nsec),11,.14,1)
      CALL WHERE
      RETURN
      END
C=============================================================
      SUBROUTINE MULTIGRA(NG)
      COMMON /GRABLOCK/X(201),Y(10,201),Z(10,201)
      DIMENSION YG(201), YM(5)
      DATA YM/5*0./
C-------------------------------SCALING----
      DO 3 J=1,NG
      DO 3 I=1,201
    3 YM(J)=AMAX1(YM(J),Y(J,I))
C
      DO 5 I=1,201
      DO 4 J=1,NG
    4 Y(J,I)=Y(J,I)/YM(J)
    5 X(I)=X(I)*1.E9
C-------------------------------PLOT----
      CALL PINIT(1.5, 5., 1000)
      DO 7 I=1,201
    7 YG(I)=Y(1,I)
      CALL MGRPHL(X,YG,201,X(1),X(201), 0., 1., 6., 4.)
      IF(NG.EQ.1) GO TO 999
C
      DO 6 J=2,NG
      DO 8 I=1,201
    8 YG(I)=Y(J,I)
    6 CALL DATPL2(X,YG,201,0,1,0,0.,0,2,0)
      CALL TITLE(1HL,5HFs(t),5,.14,1)
      CALL TITLE(1HB,11HTIME (nsec),11,.14,1)
      CALL WHERE
  999 RETURN
      END
```

REFERENCES

[1] M. W. Fitzmaurice, P. O. Minott, J. B. Abshire, and H. E. Rowe, Prelaunch Testing of the Laser Geodynamic Satellite (LAGEOS), Instrument Division, Goddard Space Flight Center, Greenbelt, Maryland, March 1977.

[2] K. E. Im, and C. S. Gardner, "Estimation of the differential pulse propagation times in two-color laser ranging systems," J. Opt. Soc. Am. A:, 3, 143-156, January 1986.

[3] R. S. Iyer, "Arrival times of satellite-broadened laser pulses," IEEE Trans. Aerospace and Electron. Syst., AES-12, 5, 577-582, September 1976.

[4] A. Papoulis, "Estimation of the average density of a nonuniform Poisson process," IEEE Trans. Commun., COM-22, 162-167, February 1974.

[5] Ref.[2] has an errata in the expression of $C_s(t_1,t_2)$, it has been corrected in this report as $f_s((t_1+t_2)/2,\ \sigma_s)$ in Eq.(8).

[6] P. M. Woodward, Probability and Information Theory with Applications to Radar, London: Pergamon, 1957, chapters 5 and 6.

[7] G. H. Song, and C. S. Gardner, "Lidar cross section of a cube-corner retroreflector," Part I of this report, Lab. Rep., Electro-Optic Systems Laboratory, Department of Electrical and Computer Eng., Univ. of Illinois at Urbana-Champaign.

VITA

G. Hugh Song was born in Seoul, Korea in 1957. He received the B.S. degree with honors in electrical engineering from the Seoul National University in 1980, and the M.S. degree in electrical engineering in 1982 from the Korea Advanced Institute of Science and Technology (KAIST).

From 1982 to 1985, he worked on fiber optics and integrated optics in Applied Optics Laboratory at KAIST. He is now a Ph.D. candidate in electrical engineering at the University of Illinois at Urbana-Champaign. He has been engaged in research on inverse scattering in integrated optics, birefringence in optical fibers, laser ranging with a cube-corner retroreflector array, device simulation of semiconductor lasers, etc.

Mr. Song is a member of the Korea Institute of Electronic Engineers and of the American Physical Society.

CUMULATIVE LIST OF RADIO RESEARCH LABORTORY

AND ELECTRO-OPTIC SYSTEMS LABORTORY REPORTS

PREPARED UNDER NASA GRANT NSG-5049

RRL Rep. No. 469 - Gardner, C. S. and N. N. Rao (December 1975), The Effects of Random Path Fluctuations on the Accuracy of Laser Ranging Systems.

RRL Rep. No. 471 - Zanter, D. L., C. S. Gardner and N. N. Rao (January 1976), The Effects of Atmospheric Refraction on The Accuracy of Laser Ranging Systems.

RRL Rep. No. 477 - Gardner, C. S. and J. R. Rowlett (November 1976), Atmospheric Refraction Errors in Laser Ranging Data.

RRL Rep. No. 478 - Hendrickson, B. E. and C. S. Gardner (December 1976), Correction of Laser Ranging Data for the Effects of Horizontal Refractivity Gradients.

RRL Rep. No. 481 - Gardner, C. S. (February 1977), Statistics of the Residual Refraction Errors in Laser Ranging Data.

RRL Rep. No. 486 - Gardner, C. S. (July 1977), Comparison Between the Refraction Error Covariance Model and Ray Tracing.

RRL Rep. No. 488 - Gardner, C. S. (September 1977), Speckle Noise in Satellite Based Lidar Systems.

RRL Rep. No. 495 - Gardner, C. S. and G. S. Mecherle (April 1978), Speckle Noise in Direct-Detection Lidar Systems.

RRL Rep. No. 496 - Gardner, C. S. and A. M. Saleh (October 1978), Speckle Noise in Differential Absorption Lidar Systems.

RRL Rep. No. 499 - Gardner, C. S. (January 1979), A Technique for Remotely Measuring Surface Pressure from a Satellite Using a Multicolor Laser Ranging System.

RRL Rep. No. 502 - Palluch, E., J. D. Shelton and C. S. Gardner (May 1979), Operating Manual for the RRL 8 Channel Data Logger.

RRL Rep. No. 505 - Gardner, C. S. and R. Axford, Jr. (March 1980), Regression Models for Multicolor Satellite Laser Ranging.

RRL Rep. No. 510 - Gardner, C. S. (April 1981), Analysis of Target Signatures for Laser Altimeters.

RRL Rep. No. 511 - Gardner, C. S. (June 1981), Atmospheric Refraction Effects in Air Borne Laser Ranging.

RRL Rep. No. 514 - Tsai, B. and C. S. Gardner (December 1981), Remote Sensing of Sea State by Laser Altimeters.

RRL Rep. No. 518 - Gardner, C. S. (August 1982), Optical Communications.

RRL Rep. No. 519 - Im, K. E. and C. S. Gardner (September 1982), Atmospheric Effects on Baseline Error in Satellite Laser Ranging Systems.

RRL Rep. No. 526 - Im, K. E., B. M. Tsai and C. S. Gardner (September 1983), Analysis of Short Pulse Laser Altimetry Data Obtained over Horizontal Path.

RRL Rep. No. 527 - Tsai, B. M. and C. S. Gardner (March 1984), Theoretical and Experimental Analysis of Laser Altimeters for Barometric Measurements Over the Ocean.

EOSL Rep. No. 84-001 - Lafaw, D. A. and C. S. Gardner (August 1984), Timing Performance of Phase-Locked Loops in Optical Pulse Position Modulation Communication Systems.

EOSL Rep. No. 85-002 - Im, K. E. and C. S. Gardner (April 1985), Estimation of the Differential Pulse Propagation Times in Two-Color Laser Ranging Systems.

EOSL Rep. No. 85-003 - Chen, C. C. and C. S. Gardner (May 1985), Phase-Locked Loop Synchronization for Direct Detection Optical PPM Communication Systems.

EOSL Rep. No. 85-006 - Im, K. E. and C. S. Gardner (August 1985), Theoretical and Experimental Analysis of the Performance of Two-Color Laser Ranging Systems.

EOSL Rep. No. 87-002 - Chen, C. C. and C. S. Gardner (March 1987), Comparison of Direct and Heterodyne Detection Optical Intersatellite Communication Links.

EOSL Rep. No. 87-003 - Natarajan, S. and C. S. Gardner (May 1987), Phase Error Statistics of a Phase-Locked Loop Synchronized Direct Detection Optical PPM Communication System.

EOSL Rep. No. 87-004 - G. Hugh Song and C. S. Gardner (June 1987), Single-Color Laser Ranging with a Cube-Corner-Retroreflector Array.

PAPERS PUBLISHED

C. S. Gardner, "Effects of Random Path Fluctuations on the Accuracy of Laser Ranging Data," Applied Optics, 15, 2539-2545, October 1976.

C. S. Gardner, "Effects of Horizontal Refractivity Gradients on the Accuracy of Laser Ranging to Satellites," Radio Science, 11, 1037-1044, December 1976.

C. S. Gardner, "Correction of Laser Tracking Data for the Effects of Horizontal Refractivity Gradients," Applied Optics, 16, 2427-2432, September 1977.

C. S. Gardner, R. Rowlett and B. E. Hendrickson, "Ray Tracing Evaluation of a Technique for Correcting the Refraction Errors in Satellite Tracking Data," Applied Optics, 17, 3143-3145, October 1978.

C. S. Gardner, "Technique for Remotely Measuring Surface Pressure from a Satellite Using a Multicolor Laser Ranging System," Applied Optics, 18, 3184-3189, September 1979.

C. S. Gardner, "Target Signatures for Laser Altimeters: An Analysis," Applied Optics, 21, 448-453, February 1982.

B. M. Tsai and C. S. Gardner, "Remote Sensing of Sea State Using Laser Altimeters," Applied Optics, 21, 3932-3940, November 1982.

C. S. Gardner, B. M. Tsai and J. B. Abshire, "Remote Sensing of Atmospheric Pressure and Sea State from Satellites Using Short-Pulse Multicolor Laser Altimeters," Proceedings of NATO-AGARD Symposium on Propagation Factors Affecting Remote Sensing by Radio Waves, 345, (46-1)-(46-11), Oberammergau, FRG, May 24-28, 1983.

C. S. Gardner, B. M. Tsai and K. E. Im, "Multicolor Laser Altimeters for Barometric Measurements over the Ocean: Theoretical," Applied Optics, 22, 2571-2577, September 1, 1983.

C. S. Gardner and J. B. Abshire, "Atmospheric refraction and target speckle effects on the accuracy of laser ranging systems," Proc. Int. Conf. on Laser Ranging Instrumentation, 1, 29-41, Royal Greenwich Observatory, Hearstmonceux, UK, September 24-28, 1984 (invited paper).

B. M. Tsai and C. S. Gardner, "Time-Resolved Speckle Effects on the Estimation of Laser Pulse Arrival Times," J. Opt. Soc. Amer. A., 2, 649-656, May 1985.

J. B. Abshire and C. S. Gardner, "Atmospheric Refractivity Corrections for Satellite Laser Ranging," IEEE Trans. Geosci. Remote Sensing, GE-2, 414-425, July 1985.

C. S. Gardner, "Remote Sensing of Atmospheric Pressure and Sea State Using Laser Altimetry," Proc. 1985 Int. Geosci. Remote Sensing Symps., 1, 199-206, Amherst, MA, October 7-9, 1985.

K. E. Im and C. S. Gardner, "Estimation of Differential Pulse Propagation Times in Two-Color Laser Ranging Systems," J. Opt. Soc. Amer. A., 3, 143-156, Jan. 1986.

C. C. Chen and C. S. Gardner, "Performance of Phase Locked Loop Synchronized Optical PPM Communication Systems," IEEE Trans. Comm., COM-34, 988-994, Oct. 1986.

C. C. Chen and C. S. Gardner, "Loss Factors Associated with Spatial and Temporal Tracking Error in Intersatellite PPM Communication Links," Proc. IEEE Global Telescom Conf., 3, 1392-1397, Houston, TX, Dec. 1-4, 1986.

C. C. Chen and C. S. Gardner, "Impact of Random Pointing and Tracking Errors on the Design of Coherent and Incoherent Optical Intersatellite Communication Links," IEEE Trans. Comm., to be published, 1987.

K. E. Im, C. S. Gardner, J. B. Abshire and J. F. McGarry, "Experimental evaluation of the performance of pulsed two-color laser ranging systems," J. Opt. Soc. Amer. A., to be published, 1987.